

ČESKÉ VYSOKÉ UČENÍ TECHNICKÉ V PRAZE  
Fakulta jaderná a fyzikálně inženýrská  
Katedra matematiky

VÝZKUMNÝ ÚKOL

**Voronoiova dláždění kvazikrystalů  
s dvanáctičetnou symetrií**

**Voronoi tillings of quasicrystals with  
dodecagonal symmetry**

Author: Eduard Šubert  
Supervisor: Ing. Petr Ambrož, Ph.D.  
Academic year: 2015/2016



## **Čestné prohlášení**

Prohlašuji na tomto místě, že jsem předloženou práci vypracoval samostatně a že jsem uvedl veškerou použitou literaturu.

V Praze dne June 5, 2016

.....

Eduard Šubert



Děkuji Ing. Petrovi Ambrožovi, Ph.D. a doc. Ing. Zuzaně Masákové, Ph.D. za pomoc s touto prací.



*Název práce:* **Voronoiova dláždění kvazikrystalů s dvanáctičetnou symetrií**

*Autor:* Eduard Šubert

*Obor:* Matematická informatika

*Druh práce:* Výzkumný úkol

*Vedoucí práce:* Ing. Petr Ambrož Ph.D., Katedra matematiky, FJFI ČVUT v Praze

*Abstrakt:* Práce se zabývá kvazikrystaly definovanými iracionálitou  $2 + \sqrt{3}$ . Jsou rozebrány jednorozměrné kvazikrystaly především s okny ve tvaru  $[c, d]$  a dvourozměrné kvazikrystaly s rovnoběžníkovým oknem i s oknem obecného tvaru. Pro oba případy je studována struktura kvazikrystalů pomocí konstrukce Voronoiho diagramu, nejdříve lokálně a po té globálně.

*Title:* **Voronoi tillings of quasicrystals with dodecagonal symmetry**

*Author:* Eduard Šubert

*Abstract:* Main focus of the thesis are quasicrystals defined by irrationality  $2 + \sqrt{3}$ . First one-dimensional quasicrystals are analyzed. Next two-dimensional quasicrystals with rhombic window and with a window of a general shape are analyzed also. For each case the structure is investigated with the aid of the Voronoi diagram at first locally and then globally.



# Contents

<b>Introduction</b>	<b>3</b>
<b>1 Preliminaries</b>	<b>5</b>
<b>2 One-dimensional quasicrystals</b>	<b>6</b>
<b>3 Two-dimensional quasicrystals</b>	<b>10</b>
<b>4 Generation of finite section of quasicrystal with rhombic window</b>	<b>12</b>
<b>5 Estimate of covering radius</b>	<b>13</b>
<b>6 Division of window</b>	<b>15</b>
<b>7 Cataloging Voronoi polygons for fixed rhombic window</b>	<b>16</b>
<b>8 Cataloging Voronoi polygons for all rhombic windows</b>	<b>22</b>
<b>9 Catalog of Voronoi polygons for rhombic window</b>	<b>24</b>
<b>10 Generation of finite section of quasicrystal with general window</b>	<b>49</b>
<b>11 Cataloging Voronoi polygons for fixed general window</b>	<b>49</b>
<b>12 Cataloging Voronoi polygons for all sizes of general window</b>	<b>53</b>
<b>13 Analysis of a quasicrystal with a circular window</b>	<b>53</b>
<b>Computation</b>	<b>55</b>
<b>Conclusion</b>	<b>57</b>



## Introduction

Quasiperiodic crystal, or quasicrystal, is a structure that displays some order, however it is not periodic. It fills an infinite space without having a translational symmetry. Quasicrystals however do posses rotational symmetry.

A lot of research [1, 2, 3] has been done on quasicrystals connected to the irrationality  $\tau = \frac{1+\sqrt{5}}{2}$ , also known as golden ratio. However there are other irrationalities that give rise to quasicrystal structures [5]:  $1 + \sqrt{2}$  and  $2 + \sqrt{3}$ . In this work we consider  $2 + \sqrt{3}$ .

Such quasicrystals do have some different properties in comparison with the golden ratio ones, which mostly cause the computational complexity of the algorithms used for analysis to rise significantly.

The first section covers the essentials for one-dimensional quasicrystals, which are mostly results of a previous work. Next the one-dimensional quasicrystal is fully analyzed and the analysis is applied to a certain subset of two-dimensional quasicrystals. Lastly the results of the analysis of these special two-dimensional quasicrystals are used to analyze a general two-dimensional quasicrystal.

In the end the bulk of the work is again applied to a different subset of two-dimensional quasicrystals that do exhibit a twelve-fold rotational symmetry. Unfortunately due to the already mentioned rise in computational complexity, these special cases were only studied locally, global analysis will be subject of future work.



# 1 Preliminaries

**Definition 1.1.** Roots of the following quadratic equation are denoted as  $\beta$  and  $\beta'$ .

$$x^2 = 4x - 1 \quad \beta = 2 + \sqrt{3} \doteq 3.732 \quad \beta' = 2 - \sqrt{3} \doteq 0.268$$

*Remark 1.* The numbers  $\beta$  and  $\beta'$  as defined in Definition 1.1 will represent the same values in the entire text.

Being roots of the same quadratic equation,  $\beta$  and  $\beta'$  have some interesting properties that are often used while working with quasicrystals.

**Theorem 1.2.** *Properties of the roots  $\beta$  and  $\beta'$ .*

$$\begin{aligned} \beta\beta' &= 1 & \beta^{k+2} &= 4\beta^{k+1} - \beta^k & \frac{1}{\beta} &= \beta' = 4 - \beta \\ \beta + \beta' &= 4 & \beta'^{k+2} &= 4\beta'^{k+1} - \beta'^k & \frac{1}{\beta'} &= \beta = 4 - \beta' \end{aligned}$$

**Definition 1.3.** Symbol  $\mathbb{Z}[\beta]$  denotes the smallest ring containing integers  $\mathbb{Z}$  and the irrationality  $\beta$ . Since  $\beta$  is quadratic the ring has the following simple form.

$$\mathbb{Z}[\beta] = \{a + b\beta \mid a, b \in \mathbb{Z}\}$$

*Remark 2.* Similarly, ring  $\mathbb{Z}[\beta']$  can be defined. According to Theorem 1.2 the two rings are equivalent:  $\mathbb{Z}[\beta] = \mathbb{Z}[\beta']$ .

## 1.1 Delone set and Voronoi tessellation

This section provides the definitions of a Delone set a covering radius and a Voronoi tessellation.

**Definition 1.4.** Let  $P \subset \mathbb{R}^n$  and let there exist  $R > 0$  and  $r > 0$  such that:

$$\forall x, y \in P, x \neq y : r \leq \|x - y\|$$

$$\forall z \in \mathbb{R}^n \exists x \in P : \|z - x\| \leq R$$

Then  $P$  is called **Delone** set.

For each Delone set  $P$  **covering radius** is defined as:

$$R_c = \inf\{R > 0 \mid \forall z \in \mathbb{R}^n \exists x \in P : \|z - x\| \leq R\}$$

**Definition 1.5.** Let  $P \subset \mathbb{R}^n$ ,  $P$  is a discrete set and  $x \in P$ . Then

$$V(x) = \{y \in \mathbb{R}^n \mid \forall z \in P, z \neq x : \|y - x\| \leq \|y - z\|\}$$

is called **Voronoi polygon** of  $x$  on  $P$ .

Voronoi polygon  $V(x)$  is said to belong to the point  $x$  and  $x$  is called the center of the polygon  $V(x)$ . The subset of  $P$  that directly shapes the polygon  $V(x)$  is called the domain of the polygon.

*Remark 3.* Example of a Delone set with the Voronoi tessellation can be seen in Figure 6.

**Theorem 1.6.** Let  $P \subset \mathbb{R}^n$  be a Delone set and  $R_c$  its covering radius. For any  $x \in P$  define:

$$N_x = \{z \in P \mid z \neq x \wedge \|z - x\| \leq 2R_c\}$$

Then Voronoi tile of  $x$  on  $P$  is

$$V(x) = \bigcap_{z \in N_x} \{y \in \mathbb{R}^n \mid \|y - x\| < \|y - z\|\}$$

*Remark 4.* Theorem 1.6 gives an algorithm for Voronoi polygon construction. First it limits the amount of points of  $P$  that need to be considered and also it shows that the polygon can be constructed by series of cuts between the center and each of the points from  $N_x$ .

## 2 One-dimensional quasicrystals

Theorems in this section are part of previous work. Hence they are only formulated here. Proofs can be found in [7].

To define a quasicrystal one more definition is needed. Function connecting the space of the quasicrystal with the space of the acceptance set called acceptance window.

**Definition 2.1.** Function  $\cdot' : \mathbb{Z}[\beta] \rightarrow \mathbb{Z}[\beta']$  is defined as  $(a + b\beta)' = a + b\beta'$ .

*Remark 5.* Notation is consistent with Definition 1.1:  $(\beta)' = \beta'$ .

**Definition 2.2.** Let  $\Omega \subset \mathbb{R}$  be a bounded set with non-empty interior. Then **one-dimensional quasicrystal** with the window  $\Omega$  is denoted by  $\Sigma(\Omega)$  and defined as:

$$\Sigma(\Omega) = \{x \in \mathbb{Z}[\beta] \mid x' \in \Omega\}$$

*Remark 6.*  $\Sigma(\Omega)$  where  $\Omega \subset \mathbb{R}$  always denotes one-dimensional quasicrystal.

Some properties of one-dimensional quasicrystals are crucial for the algorithms used for the analysis.

**Theorem 2.3.** Let  $\Omega, \tilde{\Omega} \subset \mathbb{R}$  and  $\lambda \in \mathbb{Z}[\beta]$ .

$$\begin{aligned} \Omega \subset \tilde{\Omega} &\Rightarrow \Sigma(\Omega) \subset \Sigma(\tilde{\Omega}) & \Sigma(\Omega) \cap \Sigma(\tilde{\Omega}) &= \Sigma(\Omega \cap \tilde{\Omega}) \\ \Sigma(\Omega + \lambda') &= \Sigma(\Omega) + \lambda & \Sigma(\Omega) \cup \Sigma(\tilde{\Omega}) &= \Sigma(\Omega \cup \tilde{\Omega}) \\ \Sigma(\beta\Omega) &= \frac{1}{\beta} \Sigma(\Omega) \end{aligned}$$

*Remark 7.* By Theorem 2.3 it is sufficient to analyze only intervals as windows. There are several possibilities of openness/closeness of these intervals. However only left-closed right-open intervals will be analyzed. That is justified by the following:

$$\begin{aligned} \Sigma((c, d)) &= \begin{cases} \Sigma([c, d)) & c \notin \mathbb{Z}[\beta] \\ \Sigma([c, d)) \setminus \{c'\} & c \in \mathbb{Z}[\beta] \end{cases} & \Sigma([c, d]) &= \begin{cases} \Sigma([c, d)) & d \notin \mathbb{Z}[\beta] \\ \Sigma([c, d)) \cup \{d'\} & d \in \mathbb{Z}[\beta] \end{cases} \\ \Sigma((c, d]) &= \begin{cases} \Sigma((c, d)) & d \notin \mathbb{Z}[\beta] \\ \Sigma((c, d)) \cup \{d'\} & d \in \mathbb{Z}[\beta] \end{cases} \end{aligned}$$

**Theorem 2.4.** Let  $\Omega \subset \mathbb{R}$  then  $\forall k \in \mathbb{Z} : \Sigma(\frac{1}{\beta^k}\Omega) = \beta^k\Sigma(\Omega)$ .

**Corollary 2.5.** From Remark 7 and Theorem 2.4 follows that only windows  $\Omega = [c, d]$  where  $d - c \in (\frac{1}{\beta}, 1]$  need to be analyzed. Such windows are called **base windows** or **windows in the base form**. Quasicrystals for all other windows can be acquired from the quasicrystals with the base windows by scaling and operations from Remark 7.

## 2.1 One-dimensional quasicrystal structure

Figure 1 suggests that the one-dimensional quasicrystal is a sequence of points. This section presents an analysis of spacing and distribution of these points.

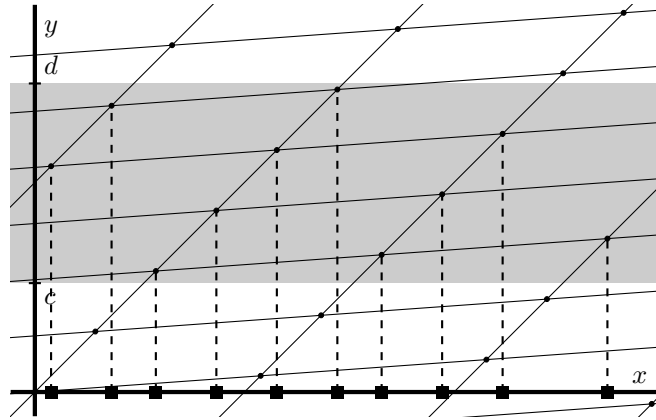


Figure 1: Illustration of one-dimensional quasicrystal. Grid intersections are defined as a set  $\{(\lambda, \lambda') | \lambda \in \mathbb{Z}[\beta]\}$ . There is a window  $\Omega = [c, d]$  on the  $y$  axis and finally the squares on the  $x$  axis are points of the quasicrystal  $\Sigma(\Omega)$ .

**Definition 2.6.** Strictly increasing sequence  $(y_n^\Omega)_{n \in \mathbb{Z}}$  defined as  $\{y_n^\Omega | n \in \mathbb{Z}\} = \Sigma(\Omega)$  where  $\Omega \subset \mathbb{R}$  is called the **sequence of quasicrystal**  $\Sigma(\Omega)$ .

**Theorem 2.7.** Let  $\Omega = [c, d]$  be a base window, then all possible distances between two consecutive points of the sequence of the quasicrystal  $(y_{n+1}^\Omega - y_n^\Omega)$  are listed in Table 1.

Window size	$\frac{1}{\beta}$	$\left(\frac{1}{\beta}, \frac{\beta-2}{\beta}\right)$	$\frac{\beta-2}{\beta}$	$\left(\frac{\beta-2}{\beta}, \frac{\beta-1}{\beta}\right)$	$\frac{\beta-1}{\beta}$	$\left(\frac{\beta-1}{\beta}, 1\right)$	1
Distances	$4\beta - 1$ $3\beta - 1$	$4\beta - 1$ $3\beta - 1$	$3\beta - 1$	$3\beta - 1$ $2\beta - 1$	$2\beta - 1$	$2\beta - 1$	$\beta$ $\beta$ $\beta$ $\beta - 1$ $\beta - 1$

Table 1: All possible distances between two consecutive points of the sequence of the quasicrystal with a window of the given size.

**Remark 8.** Please note that the cases for window sizes  $\frac{1}{\beta}$ ,  $\frac{\beta-2}{\beta}$ ,  $\frac{\beta-1}{\beta}$  and 1 each have only two different distances, therefore windows of these sizes are regarded as **singular**. Also distances for the size  $\frac{1}{\beta}$  are  $\beta$  multiples of the distances for the size 1.

**Definition 2.8.** The distances  $y_{n+1}^\Omega - y_n^\Omega$  are denoted:  $A = 4\beta - 1$ ,  $B = 3\beta - 1$ ,  $C = 2\beta - 1$ ,  $D = \beta$  and  $E = \beta - 1$ .

**Definition 2.9.** Function  $f^\Omega : \Omega \rightarrow \Omega$  for  $\Omega = [c, d)$  defined as

$$d - c \in \left( \frac{1}{\beta}, \frac{\beta-2}{\beta} \right] : f^\Omega(x) = \begin{cases} x + (\beta)' & x \in [c, d - \frac{1}{\beta}) \\ x + (4\beta - 1)' & x \in [d - \frac{1}{\beta}, c + \frac{\beta-3}{\beta}) \\ x + (3\beta - 1)' & x \in [c + \frac{\beta-3}{\beta}, d) \end{cases}$$

$$d - c \in \left( \frac{\beta-2}{\beta}, \frac{\beta-1}{\beta} \right] : f^\Omega(x) = \begin{cases} x + (\beta)' & x \in [c, d - \frac{1}{\beta}) \\ x + (3\beta - 1)' & x \in [d - \frac{1}{\beta}, c + \frac{\beta-2}{\beta}) \\ x + (2\beta - 1)' & x \in [c + \frac{\beta-2}{\beta}, d) \end{cases}$$

$$d - c \in \left( \frac{\beta-1}{\beta}, 1 \right] : f^\Omega(x) = \begin{cases} x + (\beta)' & x \in [c, d - \frac{1}{\beta}) \\ x + (2\beta - 1)' & x \in [d - \frac{1}{\beta}, c + \frac{\beta-1}{\beta}) \\ x + (\beta - 1)' & x \in [c + \frac{\beta-1}{\beta}, d) \end{cases}$$

is called the **stepping function** of the quasicrystal  $\Sigma(\Omega)$ .

**Remark 9.** Stepping function takes  $(\cdot)'$  image of a point of the quasicrystal and returns  $(\cdot)'$  image of the consecutive point.

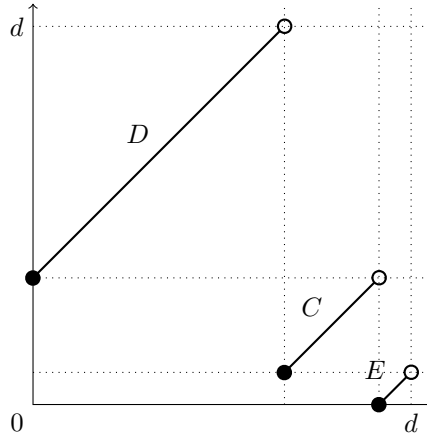


Figure 2: Graph of the stepping function for quasicrystal  $\Sigma(\Omega)$  where  $\Omega = [c, d)$ ,  $c = 0$ ,  $d = 12 - 3\beta$ ,  $C = 2\beta - 1$ ,  $D = \beta$  and  $E = \beta - 1$  (as in Definition 2.8).

Stepping function is a valuable tool in theoretical quasicrystal analysis and has direct practical use in quasicrystal generation. The following theorem lists several key properties of this function.

**Theorem 2.10.** Let  $\Omega \subset \mathbb{R}$ :

- $f^\Omega((y_n^\Omega)') = (y_{n+1}^\Omega)'$   $\forall n \in \mathbb{N}$
- $(f^\Omega)^{-1}((y_{n+1}^\Omega)') = (y_n^\Omega)'$   $\forall n \in \mathbb{N}$
- $f^\Omega$  is piece-wise translation
- Discontinuities of  $f^\Omega$  divide the window  $\Omega$  into intervals  $I_1, \dots, I_m$ . For all  $x_1, x_2 \in \Sigma(\Omega)$  holds that if  $x'_1, x'_2 \in I_j$  then both  $x_1$  and  $x_2$  have the same distance to the consecutive points.

**Definition 2.11.** Discontinuities of the stepping function of the quasicrystal  $\Sigma(\Omega)$ , where  $\Omega = [c, d]$  in the base form, are denoted as  $a^\Omega$  and  $b^\Omega$ .

$$\begin{aligned} d - c \in \left( \frac{1}{\beta}, \frac{\beta - 2}{\beta} \right] : & \quad a^\Omega = d - \frac{1}{\beta} \\ & \quad b^\Omega = c + \frac{\beta - 3}{\beta} \\ d - c \in \left( \frac{\beta - 2}{\beta}, \frac{\beta - 1}{\beta} \right] : & \quad a^\Omega = d - \frac{1}{\beta} \\ & \quad b^\Omega = c + \frac{\beta - 2}{\beta} \\ d - c \in \left( \frac{\beta - 1}{\beta}, 1 \right] : & \quad a^\Omega = d - \frac{1}{\beta} \\ & \quad b^\Omega = c + \frac{\beta - 1}{\beta} \end{aligned}$$

*Remark 10.* Notation from previous definition will be often used to divide a base window  $\Omega = [c, d]$  into three disjoint intervals.

$$\Omega = [c, a^\Omega) \cup [a^\Omega, b^\Omega) \cup [b^\Omega, d)$$

For singular cases where  $d - c \in \left\{ \frac{\beta - 2}{\beta}, \frac{\beta - 1}{\beta}, 1 \right\}$ ,  $a^\Omega = b^\Omega$  and the window is then divided only into two intervals  $[c, a^\Omega) \cup [a^\Omega, d)$ .

**Definition 2.12.** Let  $\Omega = [c, d]$ . The word  $(t_n^\Omega)_{n \in \mathbb{Z}}$  over the alphabet  $\{A, B, C, D, E\}$  is called the **word** of the quasicrystal  $\Sigma(\Omega)$ .

$$\begin{aligned} d - c \in \left( \frac{1}{\beta}, \frac{\beta - 2}{\beta} \right] : & \quad t_n^\Omega = \begin{cases} D & y_{n+1}^\Omega - y_n^\Omega = \beta \\ A & y_{n+1}^\Omega - y_n^\Omega = 4\beta - 1 \\ B & y_{n+1}^\Omega - y_n^\Omega = 3\beta - 1 \end{cases} \\ d - c \in \left( \frac{\beta - 2}{\beta}, \frac{\beta - 1}{\beta} \right] : & \quad t_n^\Omega = \begin{cases} D & y_{n+1}^\Omega - y_n^\Omega = \beta \\ B & y_{n+1}^\Omega - y_n^\Omega = 3\beta - 1 \\ C & y_{n+1}^\Omega - y_n^\Omega = 2\beta - 1 \end{cases} \\ d - c \in \left( \frac{\beta - 1}{\beta}, 1 \right] : & \quad t_n^\Omega = \begin{cases} D & y_{n+1}^\Omega - y_n^\Omega = \beta \\ C & y_{n+1}^\Omega - y_n^\Omega = 2\beta - 1 \\ E & y_{n+1}^\Omega - y_n^\Omega = \beta - 1 \end{cases} \end{aligned}$$

*Remark 11.* Word of the quasicrystal describes the distribution of the points of the quasicrystal.

**Definition 2.13.** Function  $C_\ell : \mathbb{N} \rightarrow \mathbb{N}$ , that assigns to  $n \in \mathbb{N}$  number of different sub-words of the length  $n$  in the word of the quasicrystal  $(t_m^\Omega)_{m \in \mathbb{Z}}$  where  $|\Omega| = \ell$  is called the **complexity** of the quasicrystal.

**Definition 2.14.** Set  $\mathcal{L}_\ell(n)$  containing all different sub-words of the length  $n$  in the word of the quasicrystal  $(t_m^\Omega)_{m \in \mathbb{Z}}$  where  $|\Omega| = \ell$  is called the **language** of the quasicrystal.

*Remark 12.* Please note that the complexity and the language of the quasicrystal are defined dependent only on the length of the window.

That concludes the analysis of the one-dimensional quasicrystal for now. Additional findings will be presented later.

### 3 Two-dimensional quasicrystals

In the following section a two-dimensional quasicrystal is defined and analyzed. Thanks to the Theorem 3.4, analysis of one-dimensional quasicrystals can be in some way applied to the two-dimensional quasicrystals as well.

**Definition 3.1.** Vectors  $\alpha_1, \alpha_2, \alpha_3$  and the set  $M$  denote the following.

$$\alpha_1 = (1, 0) \quad \alpha_2 = \left( \frac{2-\beta}{2}, \frac{1}{2} \right) \quad \alpha_3 = \left( \frac{\beta-2}{2}, \frac{1}{2} \right)$$

$$M = \mathbb{Z}[\beta]\alpha_1 + \mathbb{Z}[\beta]\alpha_2$$

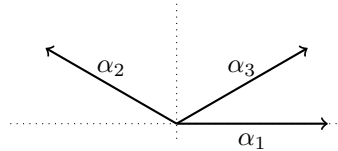


Figure 3: Plot of the three vectors  $\alpha_1, \alpha_2$  and  $\alpha_3$ .

*Remark 13.* The vectors and the set from previous definition are key to two-dimensional quasicrystal definition. The set  $M$  is used as a two-dimensional equivalent to  $\mathbb{Z}[\beta]$  from the one-dimensional quasicrystal. Function from following definition is used as a two-dimensional equivalent to  $'$ .

**Definition 3.2.** Function  $* : M \rightarrow M$  is called **star** function:

$$v^* = (a\alpha_1 + b\alpha_2)^* = a'\alpha_1 + b'\alpha_3 \quad \forall a, b \in \mathbb{Z}[\beta]$$

*Remark 14.* Simple consequence of Definition 3.2 is that  $\alpha_1^* = \alpha_1$  and  $\alpha_2^* = \alpha_3$ .

**Definition 3.3.** Let  $\Omega \subset \mathbb{R}^2$  be bounded set with nonempty interior. Then **two-dimensional quasicrystal** with the window  $\Omega$  is defined as:

$$\Sigma(\Omega) = \{x \in M \mid x^* \in \Omega\}$$

*Remark 15.*  $\Sigma(\Omega)$  where  $\Omega \subset \mathbb{R}^2$  always denotes two-dimensional quasicrystal.

*Remark 16.* The same properties from Theorem 2.3 for the one-dimensional quasicrystals apply to the two-dimensional quasicrystals as well.

To analyze the two-dimensional quasicrystals again only windows of a certain shape will be considered. That is sufficient because of Remark 16. The chosen window shape is a rhombus.

**Theorem 3.4.** Let  $I = [c, d)$ , then for the rhombus  $\Omega = I\alpha_1^* + I\alpha_2^*$  and the quasicrystal  $\Sigma(\Omega)$  it holds that:

$$\Sigma(\Omega) = \Sigma(I)\alpha_1 + \Sigma(I)\alpha_2$$

The size of the rhombus refers to the size of the interval  $|I|$  also a base rhombic window refers to a rhombic window constructed from a base window  $I$ .

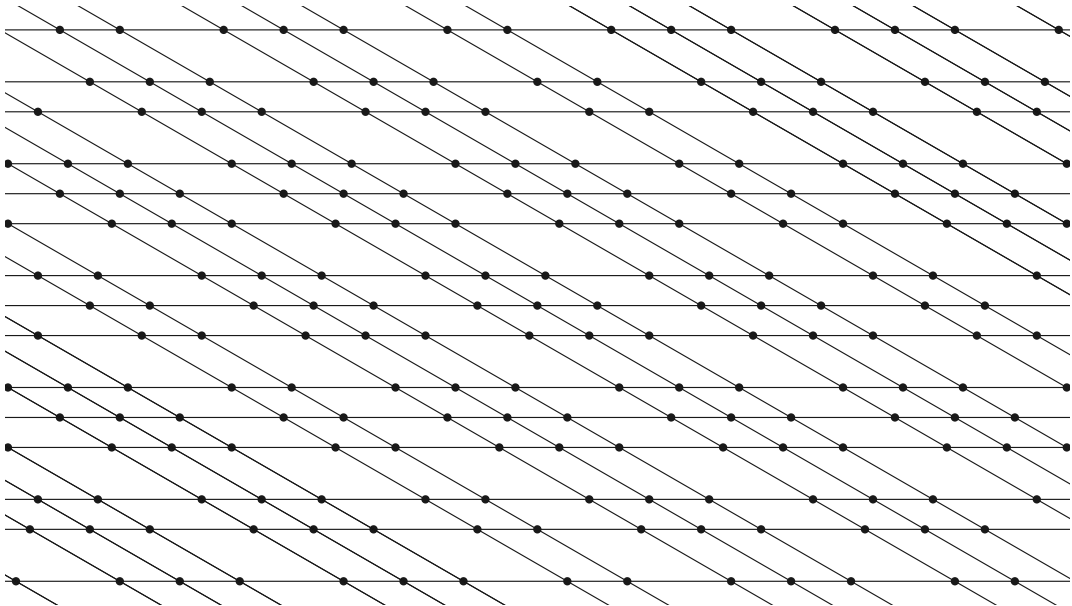


Figure 4: Illustration of the construction of the two-dimensional quasicrystal with a rhombic window from two one-dimensional quasicrystals. Horizontal lines mark copies of  $\Sigma(I)\alpha_1$  and the skewed lines mark copies of  $\Sigma(I)\alpha_2$ .

*Remark 17.* Note in the previous theorem that while  $\Omega \subset \mathbb{R}^2$  and so  $\Sigma(\Omega)$  is a two-dimensional quasicrystal,  $I \subset \mathbb{R}$  and so  $\Sigma(I)$  is a one-dimensional quasicrystal. Illustration of the construction is in the Figure 4.

From the analysis of one-dimensional quasicrystals and Theorem 3.4 it follows that the two-dimensional quasicrystals are Delone sets.

To analyze distribution of the points of a two-dimensional quasicrystal, Voronoi tessellation is used. The goal is to catalog shapes of all Voronoi tiles that appear in a quasicrystal with a rhombic window.

First an algorithm for generation of a finite section of a quasicrystal is presented.

## 4 Generation of finite section of quasicrystal with rhombic window

The algorithm for generating a finite section of a quasicrystal with a rhombic window is rather simple. Based on previous sections it uses the stepping function to generate two finite sections of one-dimensional quasicrystal and combines them to one finite section of two-dimensional quasicrystal (Theorem 3.4).

**Algorithm** The algorithm receives as an input a rhombic window  $\Omega = I\alpha_1^* + I\alpha_2^*$  and bounds  $x_1, x_2, y_1, y_2 \in \mathbb{Z}[\beta]$ . And it returns the following finite subset of the quasicrystal  $\Sigma(\Omega)$ :

$$\Sigma(\Omega) \cap ([x_1, x_2] \times [y_1, y_2])$$

First the one-dimensional interval  $I = [c, d]$  needs to be scaled and moved in such a way that it becomes a base window (Corollary 2.5) and that it contains 0:

$$(\exists k \in \mathbb{Z})(\exists \lambda \in \mathbb{Z}[\beta]) : (I = \beta^k \tilde{I} + \lambda) \wedge \left( |\tilde{I}| \in \left( \frac{1}{\beta}, 1 \right] \right) \wedge (0 \in \tilde{I})$$

Now the stepping function  $f^\Omega$  can be used to iterate from 0 and to generate enough points of the quasicrystal  $\Sigma(\tilde{I})$  to cover the bounds. However since the bounds are for the quasicrystal  $\Sigma(\Omega)$  they need to be transformed to be applicable to the quasicrystal  $\Sigma(\tilde{I})$ .

$$\begin{array}{ll} \tilde{x}_1 = x_1 & \tilde{y}_1 = 2y_1 \\ \tilde{x}_2 = x_2 + (\beta - 2)(y_2 - y_1) & \tilde{y}_2 = 2y_2 \end{array}$$

The stepping function is then used to acquire two sections of the quasicrystal  $\Sigma(\tilde{I})$ :  $\Sigma(\tilde{I}) \cap [\tilde{x}_1, \tilde{x}_2]$  and  $\Sigma(\tilde{I}) \cap [\tilde{y}_1, \tilde{y}_2]$ .

Each section needs to be transformed back:

$$\Sigma(I) = \beta^{-k} \Sigma(\tilde{I}) + \lambda'$$

and finally the finite section of the quasicrystal  $\Sigma(\Omega)$  is constructed:

$$\Sigma(\Omega) = \Sigma(I)\alpha_1 + \Sigma(I)\alpha_2$$

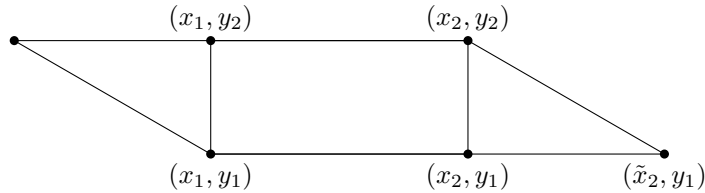


Figure 5: Illustration of how big parallelogram section of the quasicrystal (not a window) is needed to acquire a rectangular one.

*Remark 18.* Due to the way the two-dimensional quasicrystal is constructed, the result will contain more points than requested (Figure 5). However the excess points can be easily discarded.

The next goal is now to catalog all different Voronoi polygons that appear in a quasicrystal for a fixed window.

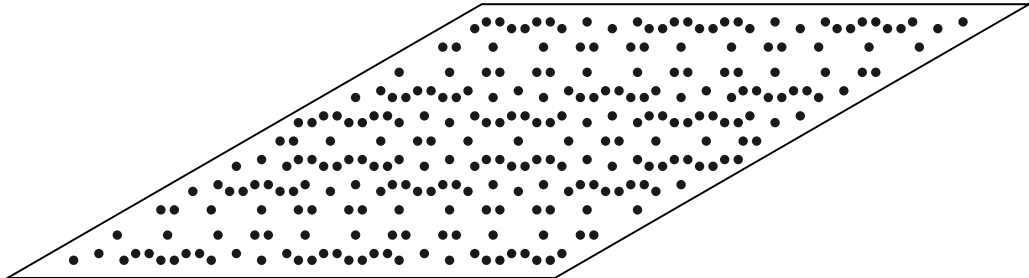
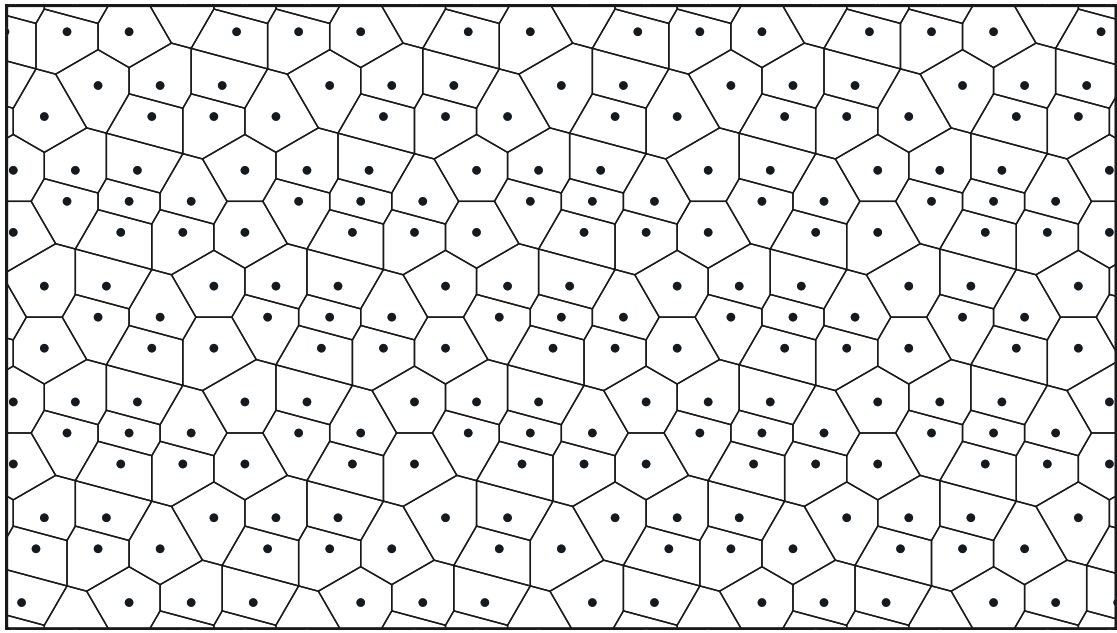


Figure 6: Finite section of the quasicrystal  $\Sigma(I\alpha_1^* + I\alpha_2^*)$  where  $|I| = \frac{6\beta - 22}{7}$  with the Voronoi tessellation and the rhombic window  $I\alpha_1^* + I\alpha_2^*$  with \* images of the points from the finite section.

## 5 Estimate of covering radius

To catalog all different tiles that appear in a quasicrystal for a fixed window, all possible local configurations of the points of the quasicrystal need to be generated.

That is achieved by generating the language of the quasicrystal  $\mathcal{L}_n$  of a sufficient length

so that the finite sections corresponding to the words from the language  $\mathcal{L}_n$  cover the disk of the radius  $2R_c$  (see the next section for more detail), where  $R_c$  is the covering radius of the quasicrystal (Definition 1.4 and Theorem 1.6).

Since the precise value of  $R_c$  is difficult to evaluate, an upper bound estimate is used instead, denoted as  $\hat{R}_c$ . As a reminder, here is the definition of the covering radius  $R_c$ , as is in Definition 1.4.

$$R_c = \inf\{R > 0 \mid z \in \mathbb{R}^n \exists x \in P : \|z - x\| \leq R\}$$

The estimate is derived from an artificial quasicrystal with only the largest distances between points (largest for the given window). Such quasicrystal has, for given window, certainly larger covering radius than any other. Since all such artificial quasicrystals are different only in scale and translation, the estimate is derived from a "normalized" one (a point in the origin and a unit distance between points).

The estimate is then evaluated as the radius of a circumscribed circle or the circumradius  $R$  of a triangle with vertices  $(0, 0)$ ,  $(-1, 0)$  and  $\left(\frac{2-\beta}{2}, \frac{1}{2}\right)$ , as in Figure 7.

$$R_c \leq R = \frac{a}{2 \sin \alpha} = \frac{1}{2 \left( \frac{1+\sqrt{3}}{2\sqrt{2}} \right)} = \frac{\sqrt{2}(\sqrt{3}-1)}{2}$$

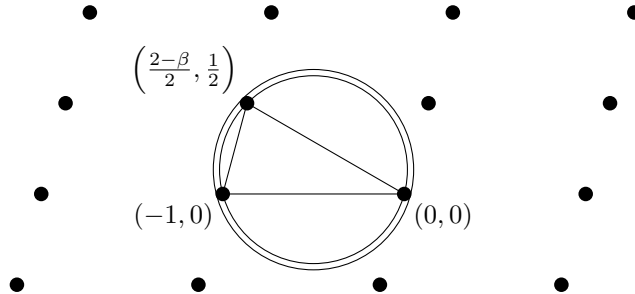


Figure 7: Section of the artificial quasicrystal with the circumcircle and a circle of the estimated radius  $\hat{R}_c$ .

Because the estimate is used in comparison with coordinates of the points of the quasicrystal, it is advantageous if it is also from  $\mathbb{Z}[\beta]$ . For that the estimate  $1.414 \doteq \sqrt{2} < 32\beta - 118 \doteq 1.426$  is used.

$$\frac{\sqrt{2}(\sqrt{3}-1)}{2} < \frac{(32\beta - 118)(\beta - 3)}{2} = 161 - 43\beta = \hat{R}_c \doteq 0.522$$

Since a normalized quasicrystal was used for the estimate, the value used in computation is the largest distance for a given window multiplied by  $\hat{R}_c$ .

*Remark 19.* There is an easier way that removes the need for such deriving. Simply estimate the covering radius with the largest distance itself. That is at first sufficient, but the case of quasicrystals with a general window forced us to use all optimizations available.

## 6 Division of window

Previous section has established that for each point of the quasicrystal, the shape of the associated Voronoi polygon is only influenced by the points of the quasicrystal that are closer than  $2L \cdot \hat{R}_c$ , where  $L$  is the largest distance for a given window.

In this section we describe the algorithm to divide one-dimensional window to parts by the same corresponding words. That is vital for two-dimensional quasicrystal analysis.

**Theorem 6.1.** *Function  $(f^\Omega)^n$  denotes the  $n$ -th iteration of the stepping function of the quasicrystal  $\Sigma(\Omega)$ . Set  $D_n = \{z_0 < z_1 < \dots < z_m\}$  contains all discontinuities of  $(f^\Omega)^n$ ,  $z_0 = c$  and  $z_m = d$ . Then  $(\forall i \in \hat{m} \cup \{0\})(\forall (y_l^\Omega)', (y_k^\Omega)' \in (z_i, z_{i+1}))$  the words  $t_l^\Omega t_{l+1}^\Omega \dots t_{l+n-1}^\Omega$  and  $t_k^\Omega t_{k+1}^\Omega \dots t_{k+n-1}^\Omega$  are the same.*

*Remark 20.* In other words the Theorem 6.1 states that the discontinuities of the  $n$ -th iteration of the stepping function divide the window into intervals of images of the points of the quasicrystal after which the same sequence of distances of the length  $n$  follow.

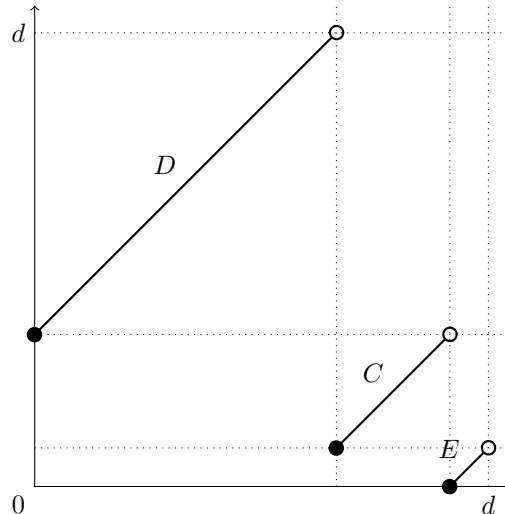


Figure 8: Graph of stepping function for quasicrystal  $\Sigma(\Omega)$  where  $\Omega = [c, d]$ ,  $c = 0$ ,  $d = 12 - 3\beta$ ,  $C = 2\beta - 1$ ,  $D = \beta$  and  $E = \beta - 1$ .

The algorithm uses the stepping function of a quasicrystal. As it is apparent from Figure 8 and Theorem 2.10, the stepping function is piece wise linear and after points of the quasicrystal corresponding to one linear segment follows the same distance to the next point of the quasicrystal. Alternatively all the points of the sequence of the quasicrystal  $y_n^\Omega$  whose images  $y_n^{\Omega'}$  are in a single interval of linearity, have the same corresponding letter in the word of the quasicrystal. That is precisely what the algorithm uses.

First, only non-singular windows are considered.

**Algorithm** Algorithm receives as an input an interval  $\Omega = [c, d]$  representing the window of the quasicrystal and  $n \in \mathbb{N}$  representing the desired length of the words.

As an output algorithm provides the division of  $\Omega$  into disjoint intervals

$$[\omega_0, \omega_1), [\omega_1, \omega_2), \dots, [\omega_{m-1}, \omega_m)$$

such that  $\omega_0 = c$  and  $\omega_m = d$ .

$$\left( \forall y_j^\Omega, y_k^\Omega \in (y_n^\Omega)_{n \in \mathbb{Z}} \right) \left( \forall i \in \widehat{m-1} : \left( (y_j^\Omega)', (y_k^\Omega)' \in [\omega_i, \omega_{i+1}] \right) \Rightarrow \left( (t_n^\Omega)_j^{j+n} = (t_n^\Omega)_k^{k+n} \right) \right)$$

The division is acquired by recursion.

For  $n = 1$  is the division already known.

$$m = 3, \omega_1 = a^\Omega, \omega_2 = b^\Omega$$

For  $n > 1$  is the division derived from the division for  $n - 1$ . Intervals

$$[\omega_0^{n-1}, \omega_1^{n-1}), [\omega_1^{n-1}, \omega_2^{n-1}), \dots, [\omega_{m-1}^{n-1}, \omega_m^{n-1})$$

denote the division for  $n - 1$ .

For each interval  $[\omega_i^{n-1}, \omega_{i+1}^{n-1})$  the stepping function image is evaluated.

$$f^\Omega([\omega_i^{n-1}, \omega_{i+1}^{n-1})) = [f^\Omega(\omega_i^{n-1}), f^\Omega(\omega_{i+1}^{n-1}))$$

Then the image is divided by the points  $a^\Omega$  and  $b^\Omega$ . If one or both of these points are inside the image, it gets divided into two or three disjoint intervals.

After all intervals for  $i \in \widehat{k-1}$  are processed, all images or their divisions are sorted and denoted  $[\omega_0, \omega_1), [\omega_1, \omega_2), \dots, [\omega_{m-1}, \omega_m)$ .

For a singular window (i. e.  $a^\Omega = b^\Omega$ ) the initial division is:

$$m = 2, \omega_1 = a^\Omega$$

At each step the image can be divided at most into two parts by the one point.

It may also be desirable to not only acquire the division of the window by the same words, but to also acquire the words themselves. That is done by a simple modification of the described algorithm. Each interval is marked with the corresponding letter  $A, B, C, D$  or  $E$  at the beginning of the recursion. While dividing the image of the interval by the points  $a^\Omega$  and/or  $b^\Omega$ , the mark is appended by an appropriate letter.

**Summary** For given  $n \in \mathbb{N}$  and window  $I = [c, d)$  the language  $\mathcal{L}_{d-c}(n)$  is finite and the described algorithm generates every word from the language. The next section takes together finite section generation, covering radius estimate and the language  $\mathcal{L}_\ell(n)$  to provide catalog of all shapes of Voronoi polygons for a given window.

## 7 Cataloging Voronoi polygons for fixed rhombic window

This section describes the algorithm for generating all Voronoi polygons in a quasicrystal with a rhombic window. Unless otherwise stated, in this section quasicrystal always means two-dimensional quasicrystal and window always means a rhombic window. The key components from previous sections are:

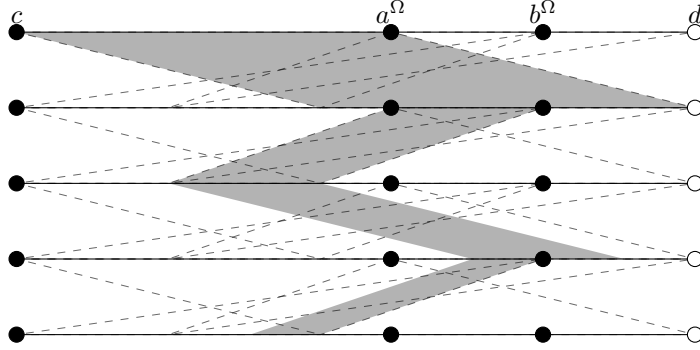


Figure 9: Iteration of the stepping function  $f^\Omega$  where  $|\Omega| = \frac{3\beta-10}{2}$ . Dashed lines show the exchange of intervals of the stepping function and the gray area shows progression of division for one interval.

1. only the points of the quasicrystal that are close enough determine the shape of the Voronoi polygon
2. finite section of the quasicrystal is easy to generate from two one-dimensional quasicrystals
3. language  $\mathcal{L}_\ell(n)$  is finite and easy to generate

There is a correspondence between a section of a word of a one-dimensional quasicrystal and a finite section of the one-dimensional quasicrystal.

$$\begin{aligned} t_m t_{m+1} \dots t_{m+k-1} t_{m+k} &\longleftrightarrow y_m, y_{m+1}, \dots, y_{m+k-1}, y_{m+k}, y_{m+k+1} \\ y_{i+1} - y_i &= t_i \end{aligned}$$

Where the last equality is in terms of the Definition 2.8.

The algorithm is then straightforward:

**Algorithm** The algorithm receives as an input a rhombic window. As an output it returns a list of Voronoi polygons found in the quasicrystal coresponding to the given window.

The largest distance within the coresponding one-dimensional quasicrystal is denoted by  $L$ .

1. evaluate  $L \cdot \hat{R}_c$  estimate of the covering radius of the quasicrystal
2. determine the length  $n$  of a word sufficient to cover the circle of radius  $2L \cdot \hat{R}_c$  (described in more detail bellow)
3. generate the language  $\mathcal{L}_\ell(n)$  (Figure 10)

BBDBDBBD	DBBDBDBD	BDBDBBDB
DBDBDBBD	DBBDBDBB	BDBBDBDB
DBDBBDBD	BDBDBDBB	BBDBDBDB

Figure 10: Example of language  $\mathcal{L}_\ell(6)$ .

4. generate finite section of one-dimensional quasicrystal for each word of the language  $\mathcal{L}_\ell(n)$ ; for each pair of one-dimensional finite sections construct finite section of the quasicrystal as in previous section and translate such that each finite section contains origin in the middle (Figure 11)
5. construct a Voronoi polygon for the origin for each finite section (Figure 12)

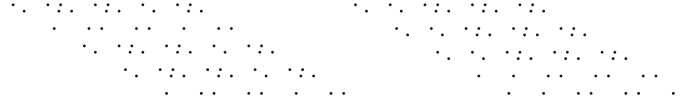


Figure 11: Example of 2 finite sections.

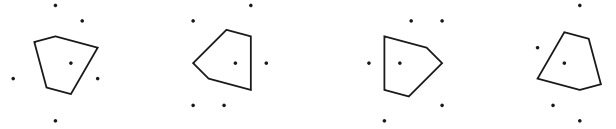


Figure 12: Example of one Voronoi polygon in four different orientations.

To justify that the algorithm finds all Voronoi polygons for a given window consider that the shape of each Voronoi polygon is determined by the points of the quasicrystal, that are distant at most  $2L \cdot \hat{R}_c$  from the center of the polygon. In other words, the shape is only determined by a finite section of the quasicrystal. Each finite section of the quasicrystal with a rhombic window is described by two finite sections of a one-dimensional quasicrystal. Each finite section of one-dimensional quasicrystal with  $n+1$  points is described by a finite word of the quasicrystal, every such word is present in the language  $\mathcal{L}_\ell(n)$ .

## 7.1 Determine sufficient $n$

Part of the algorithm that was not covered in detail is how to determine the length of a word sufficient to cover a circle of radius  $2L \cdot \hat{R}_c$ . First a rhombus is circumscribed to the circle of the radius  $2L \cdot \hat{R}_c$ . The side of such rhombus is 4 times larger than the circle radius. Then such  $n$  has to be found that a finite section of one-dimensional quasicrystal corresponding to each word from  $\mathcal{L}_\ell(n)$  has to be at least as long as the side of the circumscribed rhombus. There are several approaches, two are described here.

One way is to get the smallest distance  $S$  for the one-dimensional quasicrystal and set  $n = \lceil \frac{8L \cdot \hat{R}_c}{S} \rceil$ .

The second way is to start with  $n = 2$ , test each word of the language  $\mathcal{L}_\ell(n)$  and increase by 1 until  $n$  is sufficient.

The second way takes more time to compute but produces better estimate, which will be desirable once analyzing quasicrystals with a general window.

## 7.2 Different orientations

As it is apparent from Figure 12, the same shape of a Voronoi polygon can appear in the quasicrystal in several orientations. This section covers the analysis of different orientations of

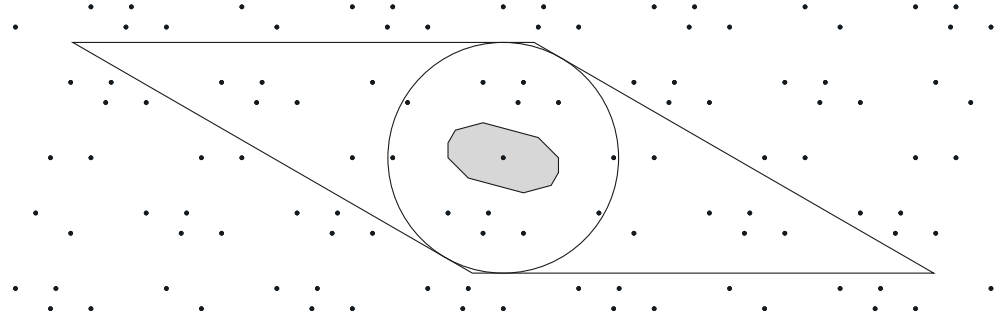


Figure 13: Finite section of a quasicrystal containing the origin. The circle has a radius  $2L \cdot \hat{R}_c$  and contains all the points of the quasicrystal that determine the shape of the Voronoi polygon for the origin. The circumscribed rhombus contains a superset.

Voronoi polygons.

It is helpful to see the connection between the domain of the Voronoi polygon and its \* image in the window of the quasicrystal. Figure 14 shows a Voronoi polygon from the quasicrystal with the window size  $2 - 7\beta$ , the window and \* image of its domain and its center.

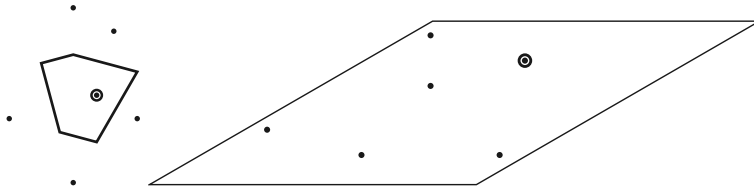


Figure 14: A Voronoi polygon with its center and domain and the \* image in the window of the quasicrystal.

It is clear that a Voronoi polygon can appear in a quasicrystal only if the \* image of its domain and center fits inside the window. Therefore a section of the window can be associated with a Voronoi polygon through its center. The section shows where in the window the \* image of the center can be so that the \* image of the domain fits in also (Figure 15).

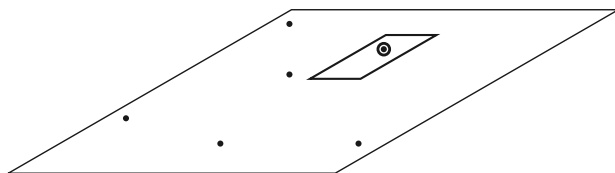


Figure 15: A window with the \* image of the domain and the center from the Figure 14 with the associated section.

In fact the entire window can be divided in such sections. Every point of the quasicrystal whose \* image falls within one section is the center of a Voronoi polygon of the same shape (Figure 16). The algorithm for producing such division will be covered in the next section.

From the division two axis of symmetry are apparent. These are the sources of the different orientations of the Voronoi polygons of the same shape. The highlighted sections in the Figure

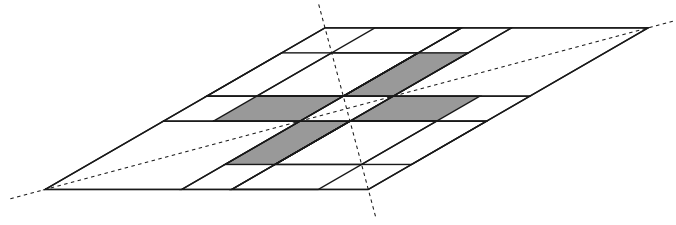


Figure 16: A window with the division into sections by the shape of corresponding Voronoi polygon.

16 correspond to the four Voronoi polygons from the Figure 12

### 7.3 Dividing rhombic window into sections by the shape of corresponding Voronoi polygon

Algorithm for checking whether a set of points belongs to the quasicrystal also produces the shape of the section of the window.

Let  $\Omega$  be a rhombic window,  $V$  one of the Voronoi polygons in the quasicrystal  $\Sigma(\Omega)$ ,  $c \in M$  the center of  $V$ ,  $D = \{p_1, \dots, p_k\} \subset M$  the domain of  $V$  and  $q_i = p_i - c$ ,  $i \in \hat{k}$ . Then the  $*$  image of the center and the domain fit inside the window:

$$c^* \in \Omega \quad \wedge \quad c^* + q_i^* \in \Omega \quad (\forall i \in \hat{k})$$

which is equivalent to whether the image of the center  $c^*$  fits inside translated windows:

$$c^* \in \Omega \quad \wedge \quad c^* \in \Omega - q_i^* \quad (\forall i \in \hat{k})$$

$$c^* \in \bigcap_{i \in \hat{k}} (\Omega - q_i^*) \cap \Omega$$

Now first if the intersection is not empty then the polygon  $V$  appears in the quasicrystal  $\Sigma(\Omega)$ , this will be useful while analyzing quasicrystals with a general window. Also the intersection shows exactly the desired section of the window. Only if the image of the center fits inside this intersection does the image of the domain fit inside the window and that determines the shape of the Voronoi polygon.

There is however a slight caveat. The intersection might be larger than the desired section. Consider this example, in the so far analyzed quasicrystal with the window size  $2\beta - 7$  there is a polygon very similar in shape to the one in the Figure 12 (Figure 17).

The intersection is a superset of the section. The Figure 18 shows the intersections for first polygons of each line in the Figure 17.

Clearly the first intersection is a subset of the second one and also the corresponding polygons are in the same relation. Therefore a conclusion can be drawn that if the  $*$  image falls within the smaller intersection, its polygon will be the smaller one because the domain of the smaller polygon will be present in the quasicrystal. Only if the  $*$  image of the center fall outside the smaller intersection but inside the larger intersection the polygon will be the larger one (Figure 19).

Similar situation happens with the polygons in the Figure 20.

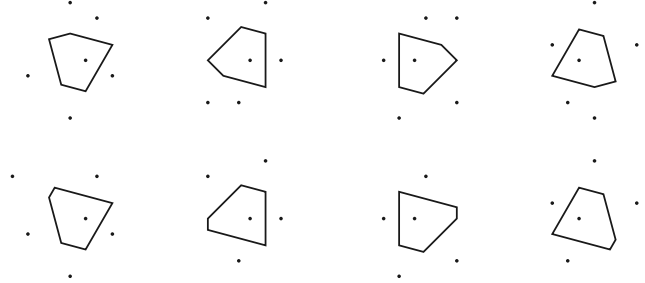


Figure 17: First line are the polygons from the Figure 12 and the second line are the slightly larger ones that also appear in the quasicrystal.

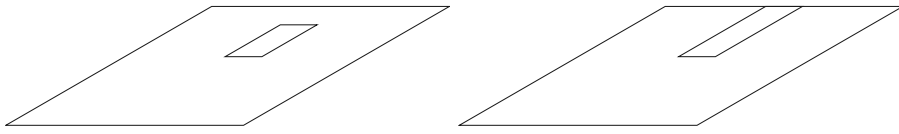


Figure 18: Intersections for first polygons in each line in the Figure 17.

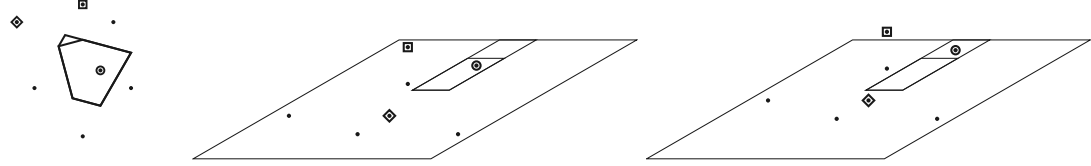


Figure 19: The points in the left window correspond to the smaller polygon, the  $\diamond$  marked point is not a member of the domain. The points in the right window correspond to the larger polygon, the  $\square$  marked point no longer fit inside the window and so the  $\diamond$  marked point becomes a member of the domain.

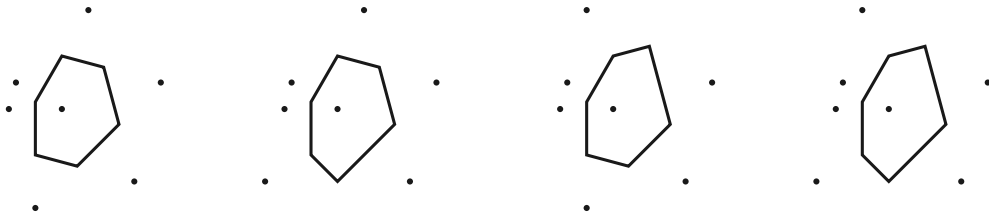


Figure 20: These Voronoi polygons also have overlapping intersections.

**Summary** This section covered the algorithms for generating all different shapes of Voronoi polygons for a fixed rhombic window and for dividing said window into sections by the different shapes. Next section will achieve the same for all rhombic window sizes.

## 8 Cataloging Voronoi polygons for all rhombic windows

To catalog all different shapes of Voronoi polygons in all quasicrystals with a rhombic window, several simplifications are put in place. First only base rhombic windows are considered since polygons from other quasicrystals are not different in shape only in scale. Secondly the base windows are divided by the same language into finitely many groups.

The proofs of the following theorems can be found in [4].

**Theorem 8.1.** Let  $\Omega = [c, c + \ell]$ .

If  $\ell \notin \mathbb{Z}[\beta]$  then  $\mathcal{C}_\ell(n) = 2n + 1$ ,  $\forall n \in \mathbb{N}$ .

If  $\ell \in \mathbb{Z}[\beta]$  then  $\exists^1 k \in \mathbb{N}$  such that  $((f^\Omega)^k(a^\Omega) = b^\Omega)$  or  $((f^\Omega)^{k+1}(b^\Omega) = a^\Omega)$  and

$$\mathcal{C}_\ell(n) = \begin{cases} 2n + 1 & \forall n \leq k \\ n + k + 1 & \forall n > k \end{cases}$$

**Theorem 8.2.**

$$\mathcal{D}_n = \left\{ \ell \mid \ell \in \left( \frac{1}{\beta}, 1 \right] \wedge \mathcal{C}_\ell(n) < 2n + 1 \right\}$$

Then elements of  $\mathcal{D}_n$  divide interval  $I := \left( \frac{1}{\beta}, 1 \right]$  into finite amount of disjoint sub-intervals  $(I_m)_{m \in \hat{N}}$  such that  $\mathcal{L}_{\ell_1}(n) = \mathcal{L}_{\ell_2}(n) \forall \ell_1, \ell_2 \in I_m, \forall m \in \hat{N}, \forall N \in \mathbb{N}$ .

*Remark 21.* Please note that  $\mathcal{D}_n$  from Theorem 8.2 divides base windows into sets by the same language whereas  $D_n$  from Theorem 6.1 divides a single window into intervals by the sequences of points that follow.

Previous two theorems give a guide to which points divide the base windows into groups of the same language and also how to find those points.

Now is the time to introduce new view on the one-dimensional base windows as a whole. Figure 21 shows a plot of all base windows side by side.

It shows well how the window changes while increasing in size and how the singular windows come to existence. However more importantly it shows that  $\mathcal{D}_1 = \left\{ \frac{\beta-2}{\beta}, \frac{\beta-1}{\beta}, 1 \right\}$ . The algorithm for generating  $\mathcal{D}_n$  is very similar to the algorithm for division of a fixed window or the algorithm for generating  $D_n$ . Only this time instead of getting a stepping function image of the endpoints of a interval, the function is used on the whole line segments representing  $a^\Omega$  and  $b^\Omega$ . Every time images of these line segments intersect a new point is added to the set  $\mathcal{D}_n$ .

For a sufficient  $n$ , such  $\mathcal{D}_n$  can be constructed that the same language on the subintervals implies the same set of different shapes of Voronoi polygons on corresponding quasicrystals. The endpoints of the subintervals are then examined independently.

Such  $n$  is determined by the algorithm from the previous section. The first approach is used. For the base windows there are three combinations of the largest and smallest distance possible:  $A, D$ ;  $B, D$  and  $C, E$ . The  $n$  is determined for each and the largest one is selected.

$$n_1 = \left\lceil \frac{8A \cdot \hat{R}_c}{D} \right\rceil = 16 \quad n_2 = \left\lceil \frac{8B \cdot \hat{R}_c}{D} \right\rceil = 12 \quad n_3 = \left\lceil \frac{8C \cdot \hat{R}_c}{E} \right\rceil = 10$$

Therefore  $n = 16$  and  $\mathcal{D}_{16}$  is constructed. To generate all possible Voronoi polygons in all quasicrystals with base windows, the algorithm from the previous section is used on all rhombic

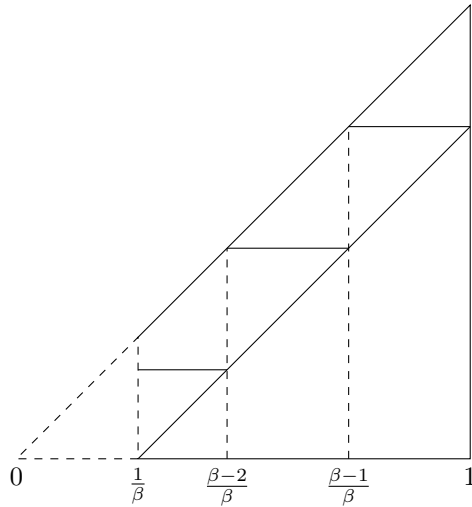


Figure 21: One-dimensional base windows. Each vertical slice represents one base window. The skewed line marks the point  $a^\Omega$  and the horizontal lines mark the point  $b^\Omega$ .

windows with a side  $\ell \in \mathcal{D}_{16}$  and for any  $\ell \in I_m$  for each of the disjoint intervals. Thus the Voronoi polygons will be analyzed for each different language  $\mathcal{L}_\ell(16)$ , which is sufficient to catalog every different Voronoi polygon.

However the resulting set of Voronoi polygons from  $\mathcal{D}_{16}$  is identical to the set of Voronoi polygons for  $\mathcal{D}_4$  and is different from the one for  $\mathcal{D}_3$ . Thus it is assumed, that the generous estimates inflated the  $n$  greatly and  $n = 4$  is sufficient.

**Summary** This section covered the method for generating a catalog of all different Voronoi polygons for all quasicrystals with base windows. Additionally it finalized the sufficient  $n$  as  $n = 4$ .

The next section will conclude the analysis of the two-dimensional quasicrystals with rhombic windows with the catalog of all different Voronoi polygons.

## 9 Catalog of Voronoi polygons for rhombic window

As concluded in the previous section the sufficient  $n = 4$ .

$$\mathcal{D}_4 = \{4 - \beta, 10\beta - 37, 19 - 5\beta, 6\beta - 22, 2\beta - 7, 8 - 2\beta, 5\beta - 18, \beta - 3, 12 - 3\beta, 4\beta - 14, 1\}$$

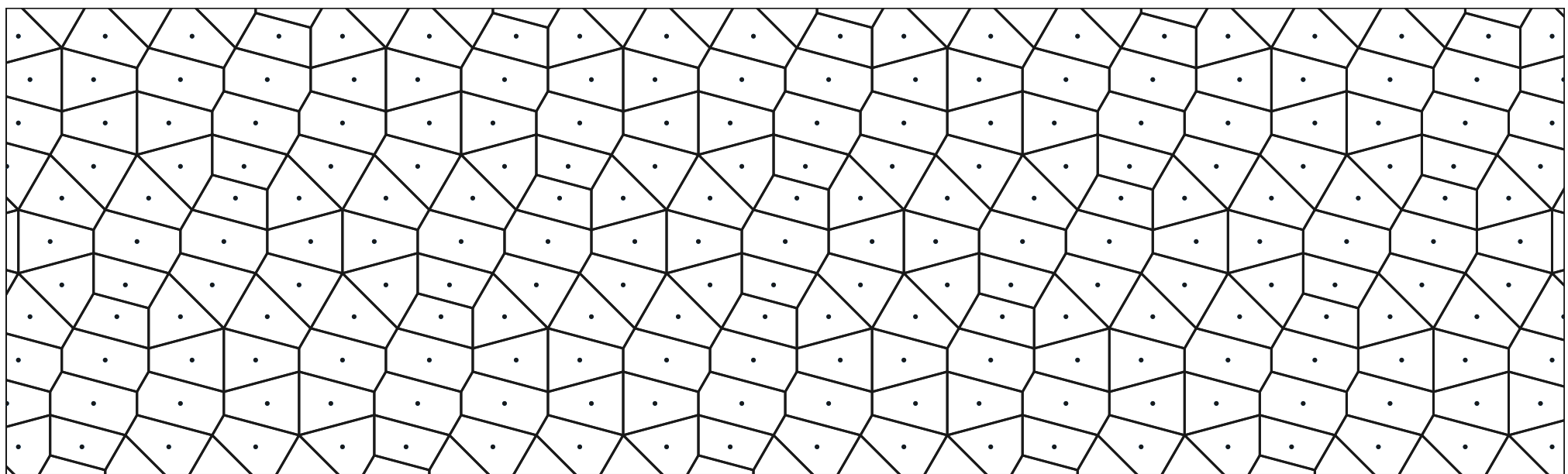
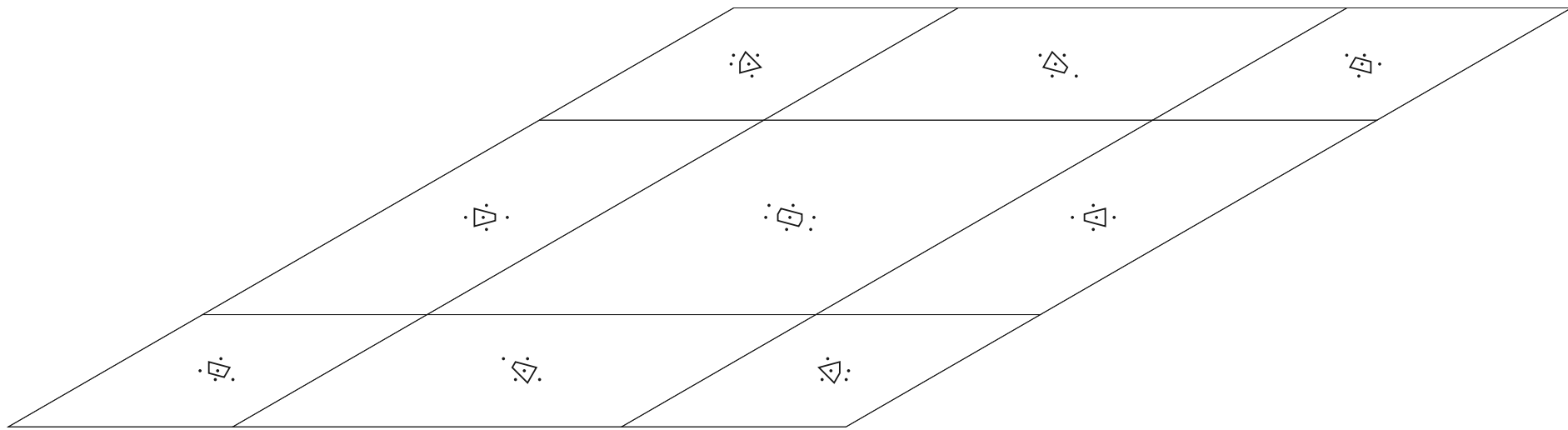
The endpoint  $4 - \beta = \frac{1}{\beta}$  is added for ease of use. To get the full set of sizes of rhombic windows that need to be analyzed a mean of each two consecutive numbers from  $\mathcal{D}_4$  is added. These represent the intervals of the same language.

$$\mathcal{D} = \left\{ 4 - \beta, \frac{9\beta - 33}{2}, 10\beta - 37, \frac{5\beta - 18}{2}, 19 - 5\beta, \frac{\beta - 3}{2}, 6\beta - 22, \frac{8\beta - 29}{2}, 2\beta - 7, \frac{1}{2}, 8 - 2\beta, \frac{3\beta - 10}{2}, 5\beta - 18, \frac{6\beta - 21}{2}, \beta - 3, \frac{9 - 2\beta}{2}, 12 - 3\beta, \frac{\beta - 2}{2}, 4\beta - 14, \frac{4\beta - 13}{2}, 1 \right\}$$

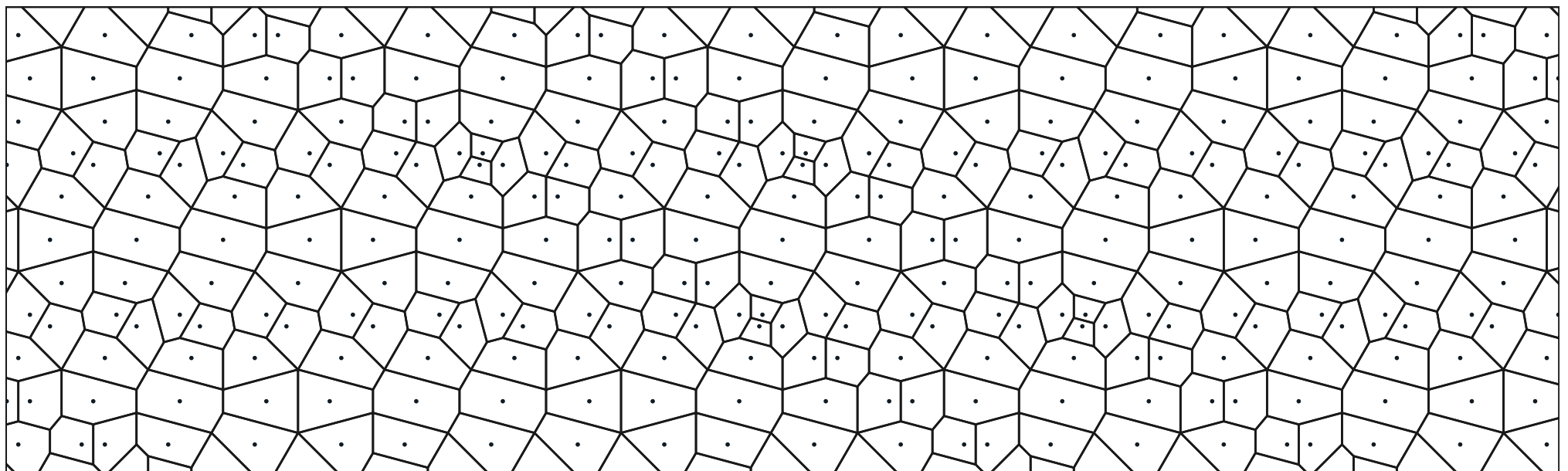
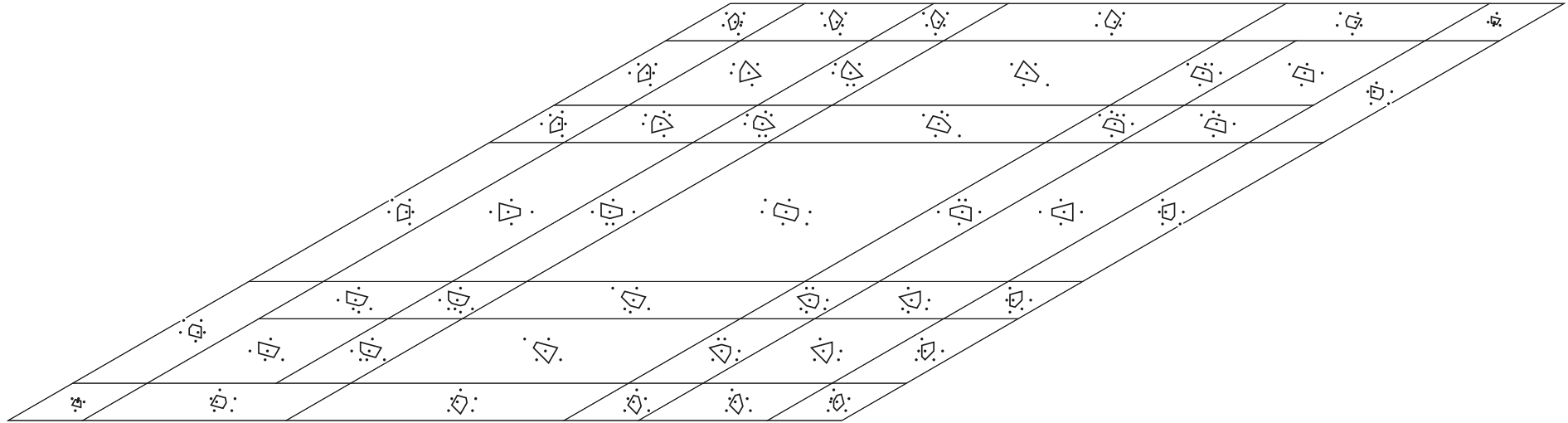
Following is a list of windows for each size in  $\mathcal{D}$  divided in sections by the corresponding Voronoi polygon accompanied by a finite section of corresponding quasicrystal. The window for 1 looks identical as the window for  $4 - \beta$  because  $\beta\Sigma(\Omega^1) = \Sigma(\Omega^{4-\beta})$ .

The windows have been scaled to fit the page therefore the size of the polygons seem to decrease with growing window size. The finite sections of the quasicrystals do have the same scale.

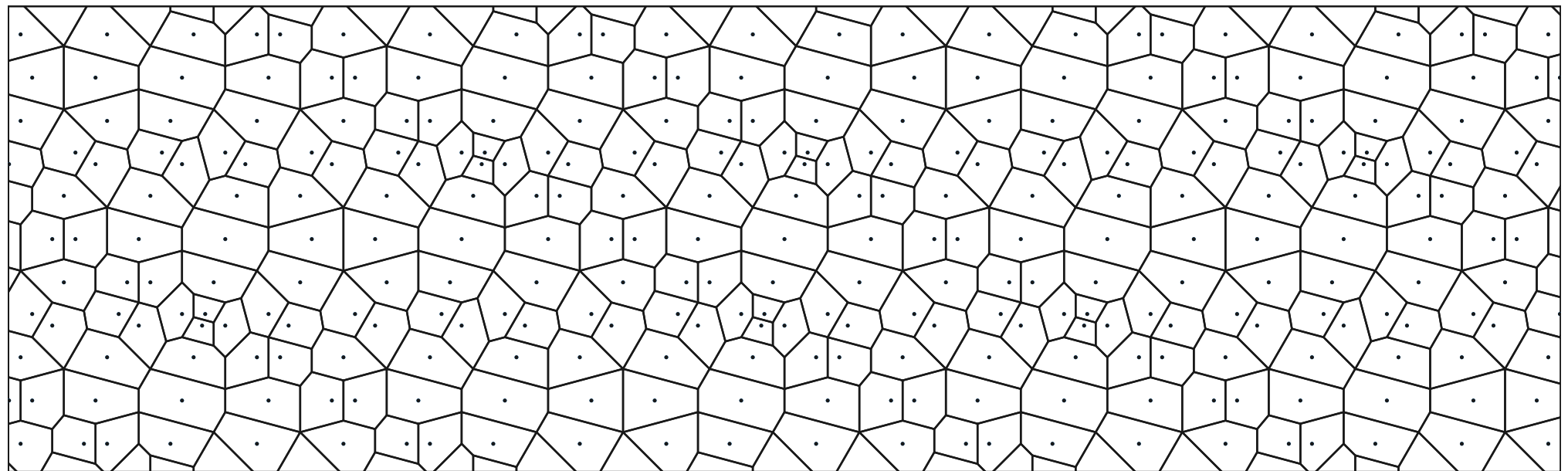
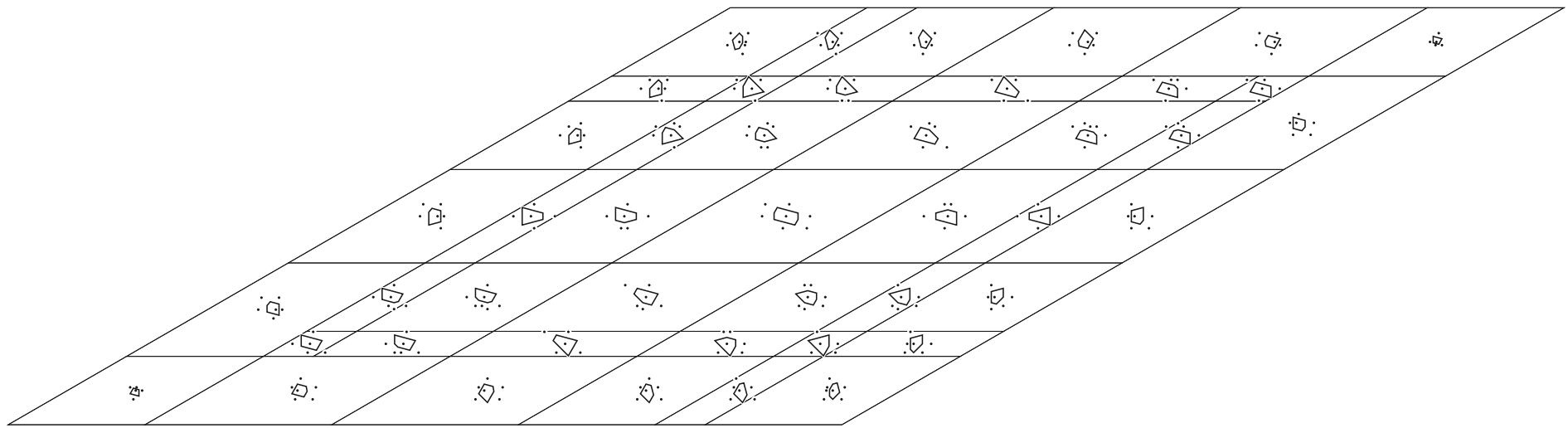
The catalog is then concluded by a list of all Voronoi polygons for quasicrystals with base windows and a table assigning the polygons to the quasicrystals. In the list for each polygon only one orientation is selected if more are available.



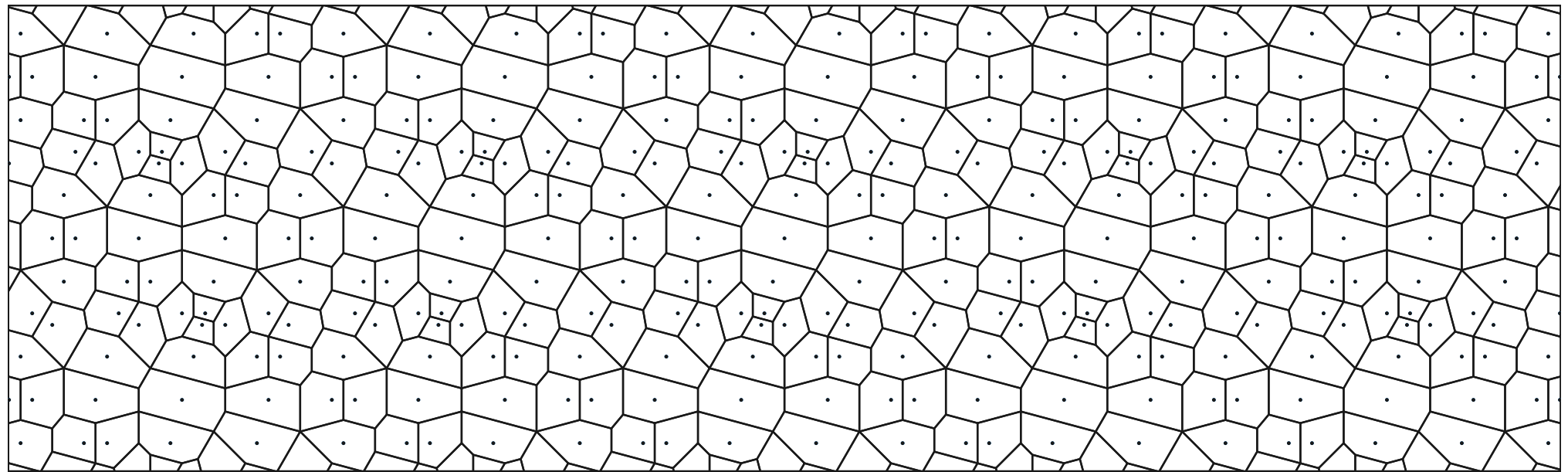
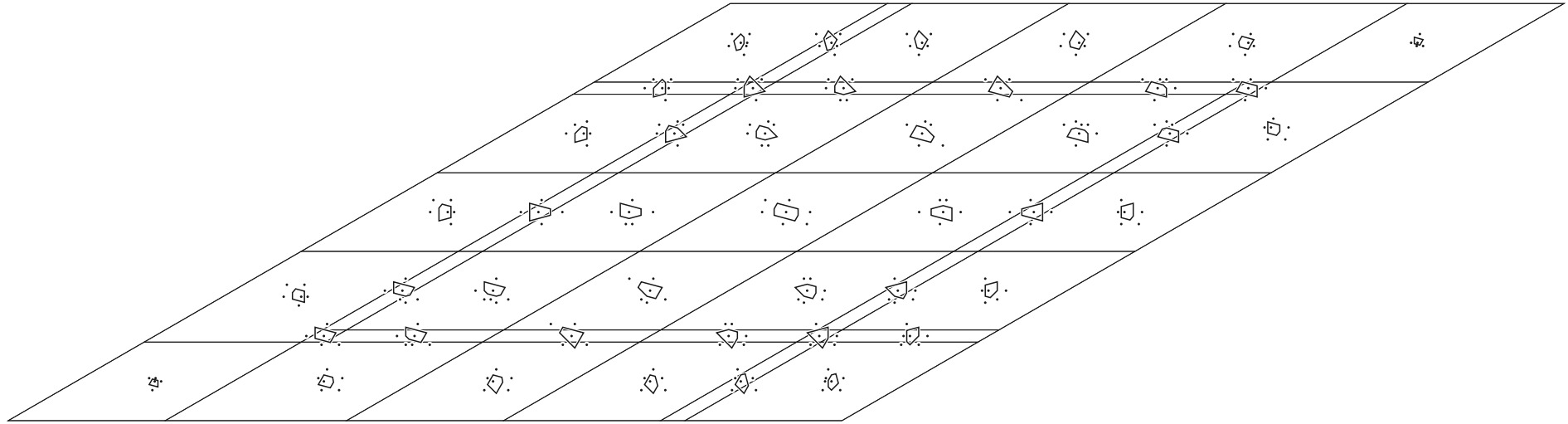
window size:  $4 - \beta$



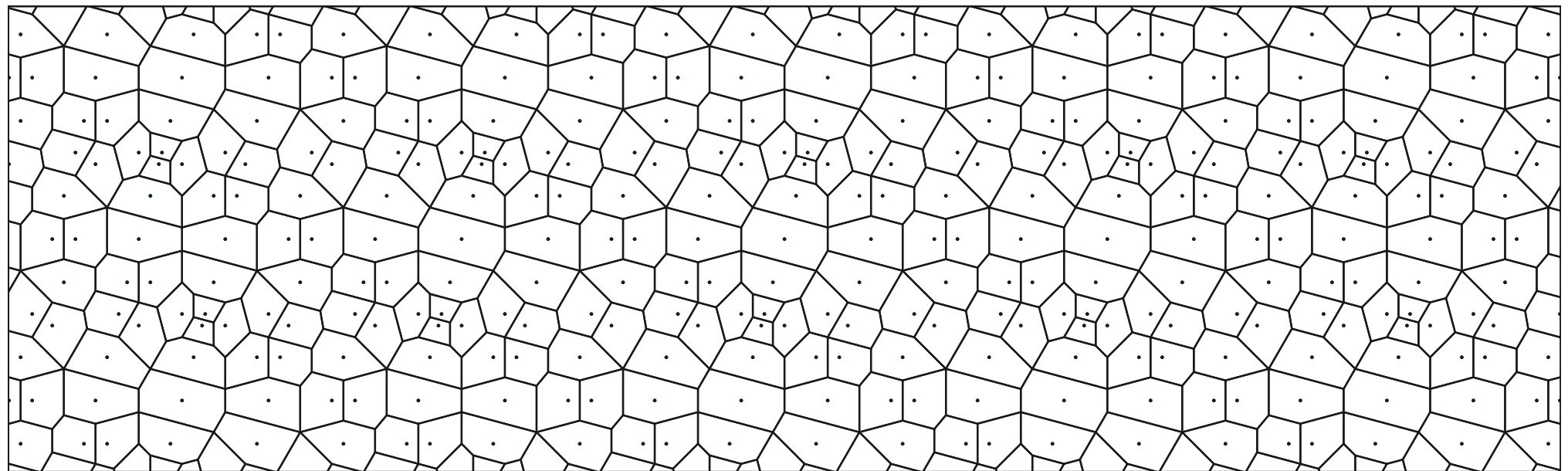
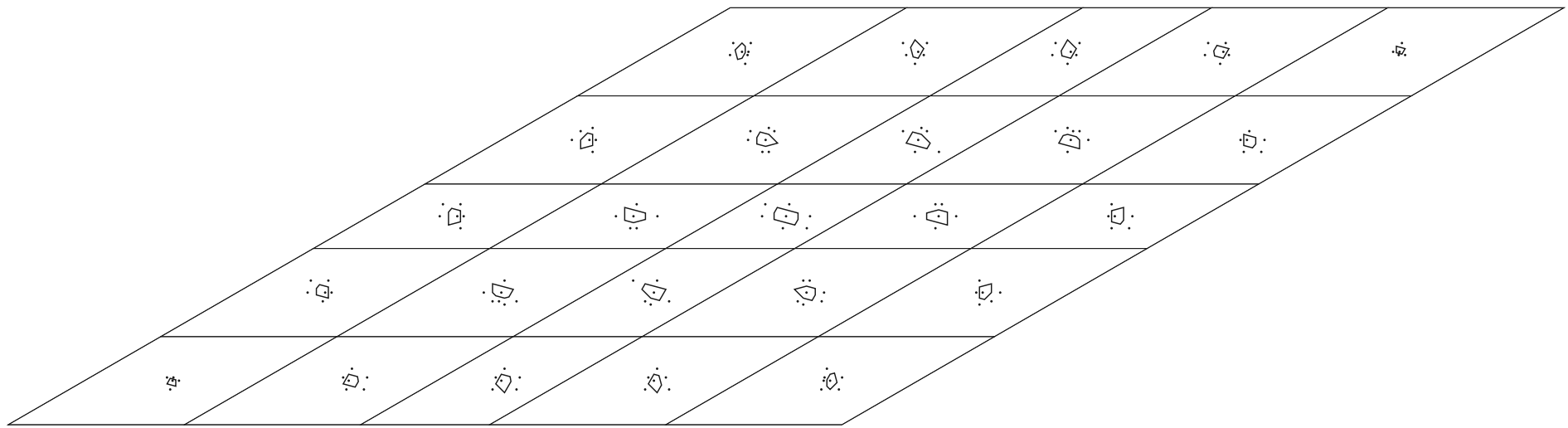
window size:  $\frac{9\beta-33}{2}$



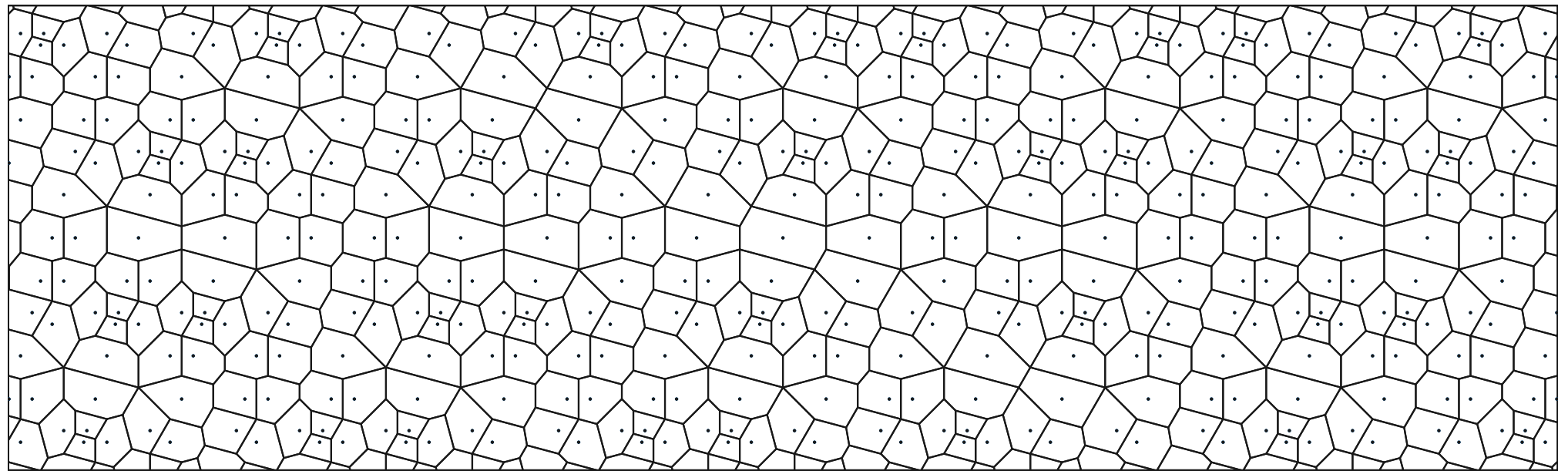
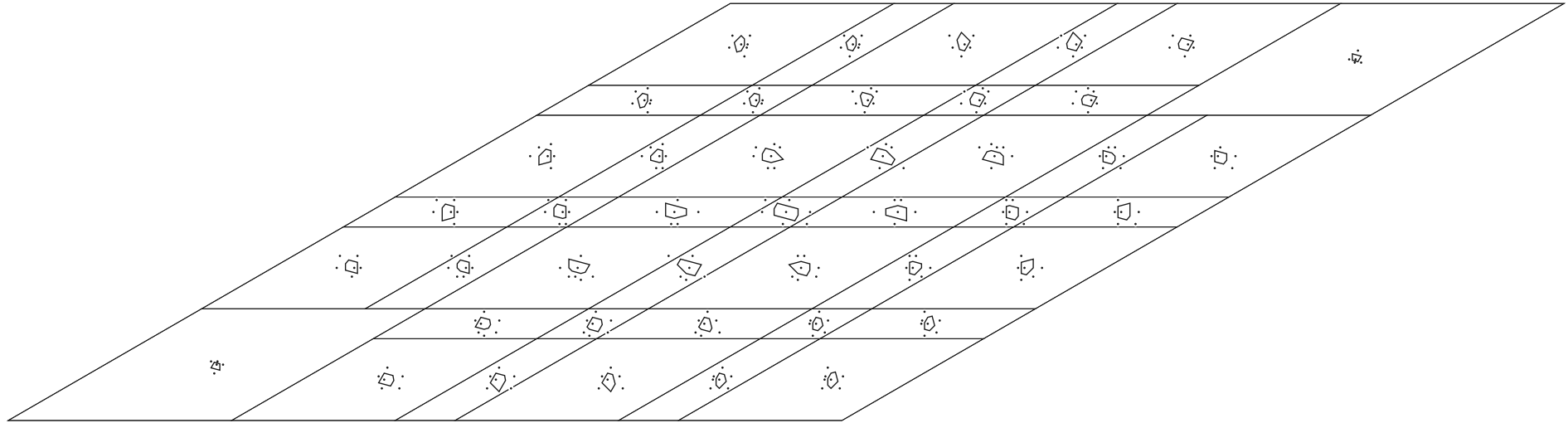
window size:  $10\beta - 37$



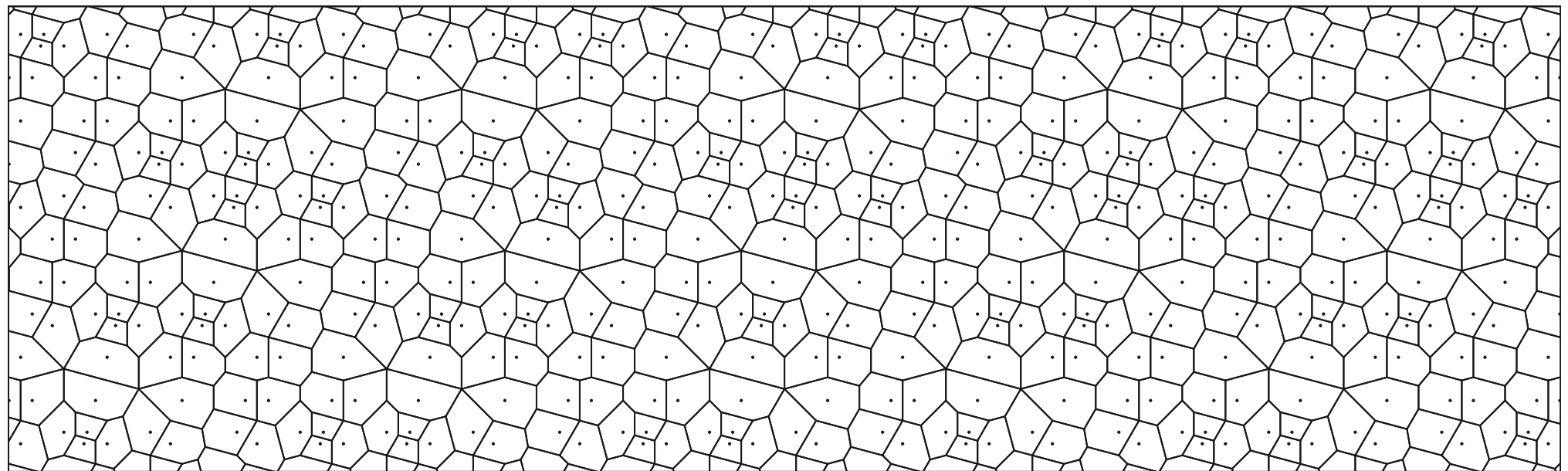
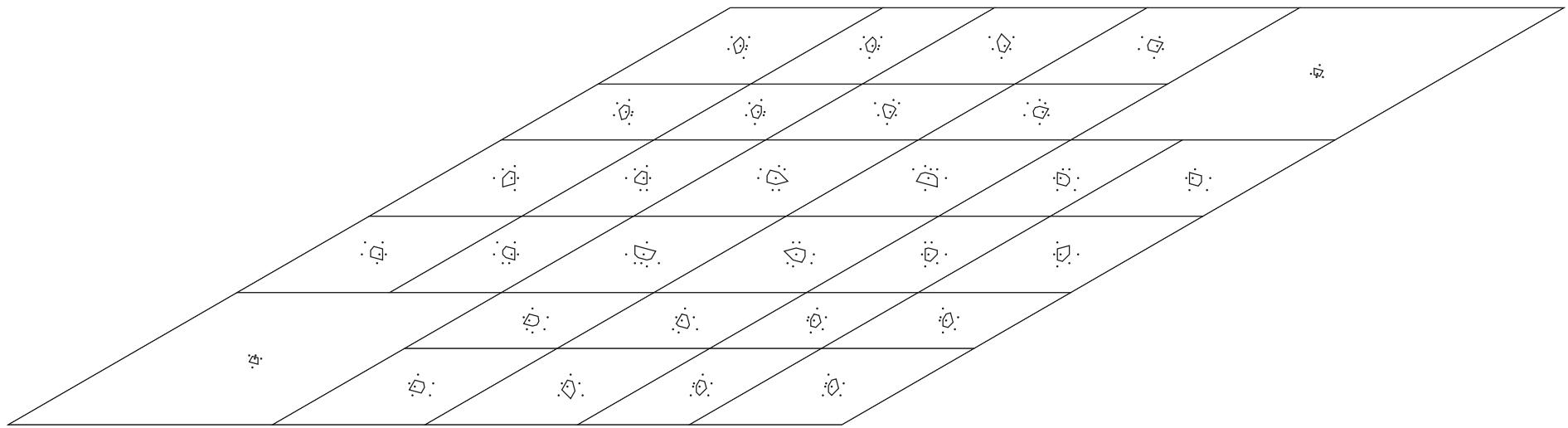
window size:  $\frac{5\beta-18}{2}$



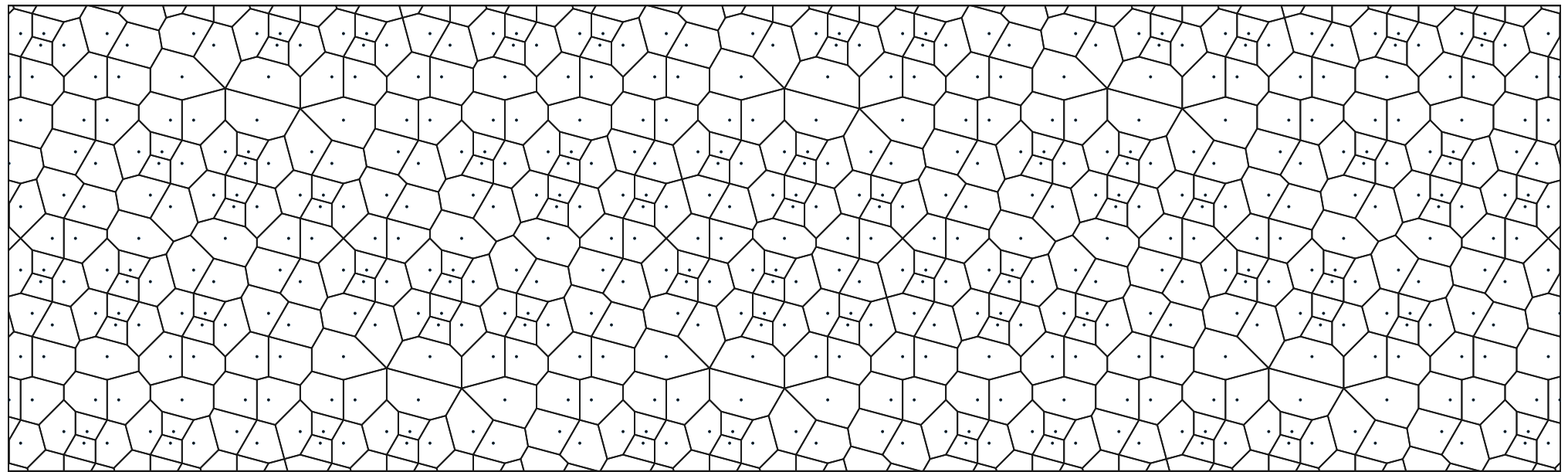
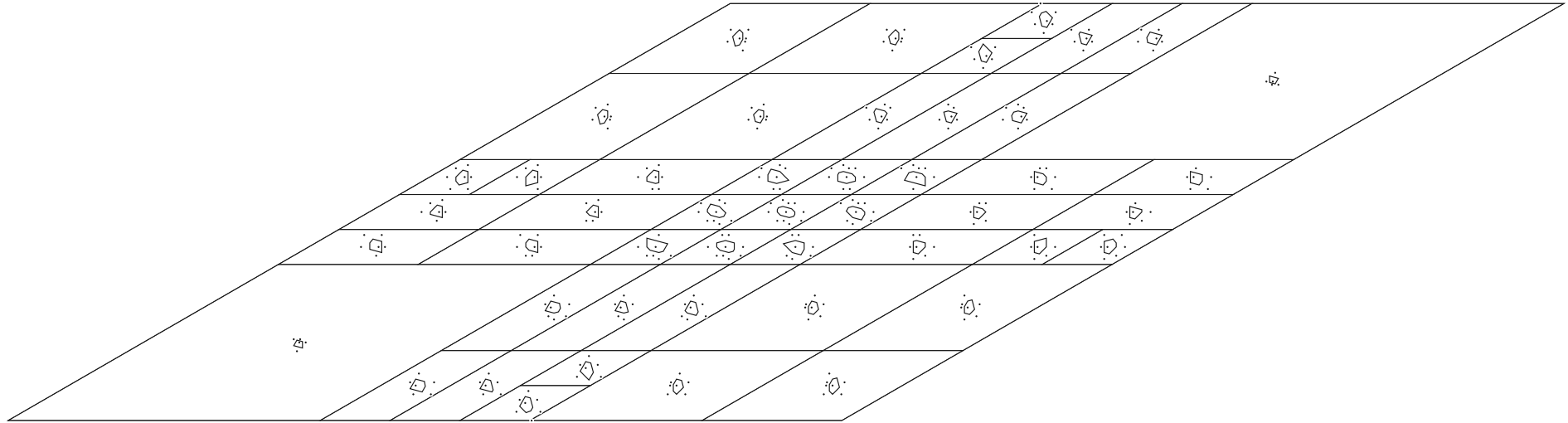
window size:  $19 - 5\beta$



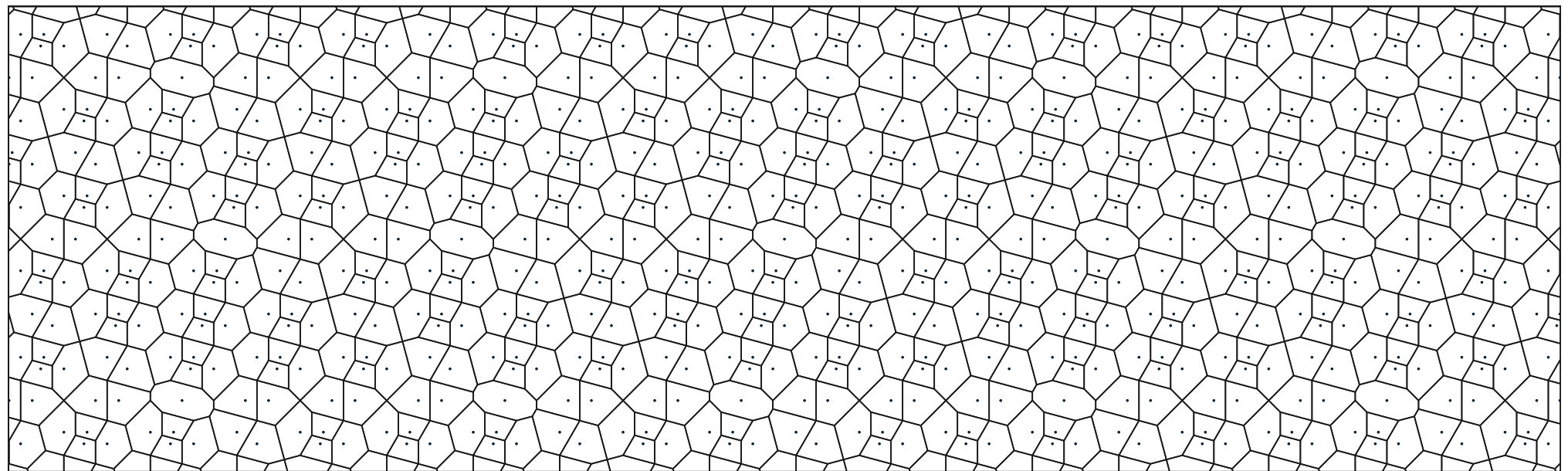
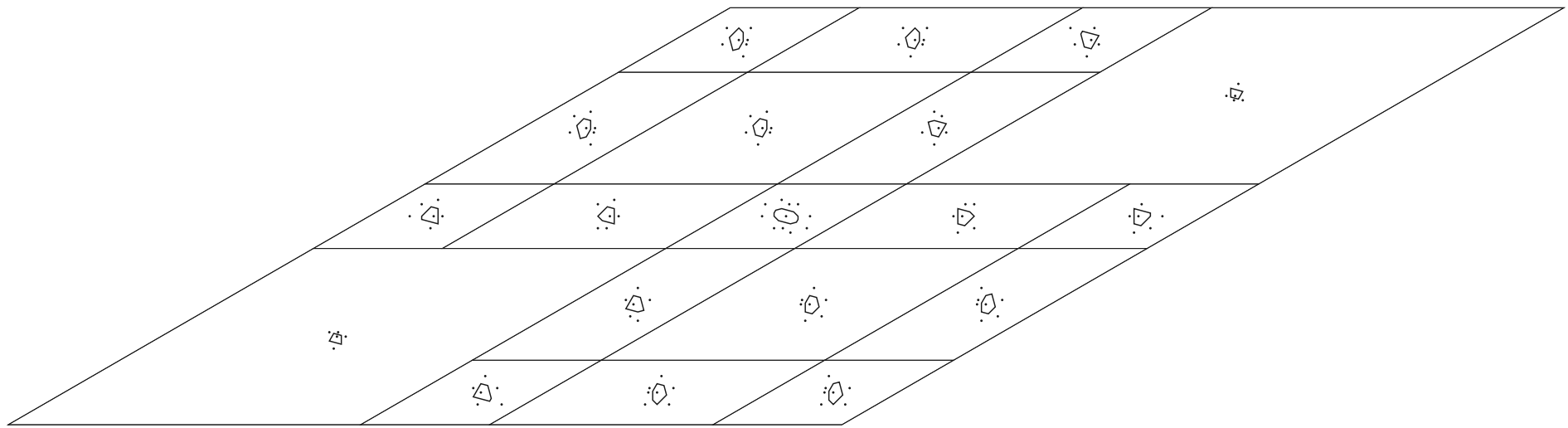
window size:  $\frac{\beta-3}{2}$



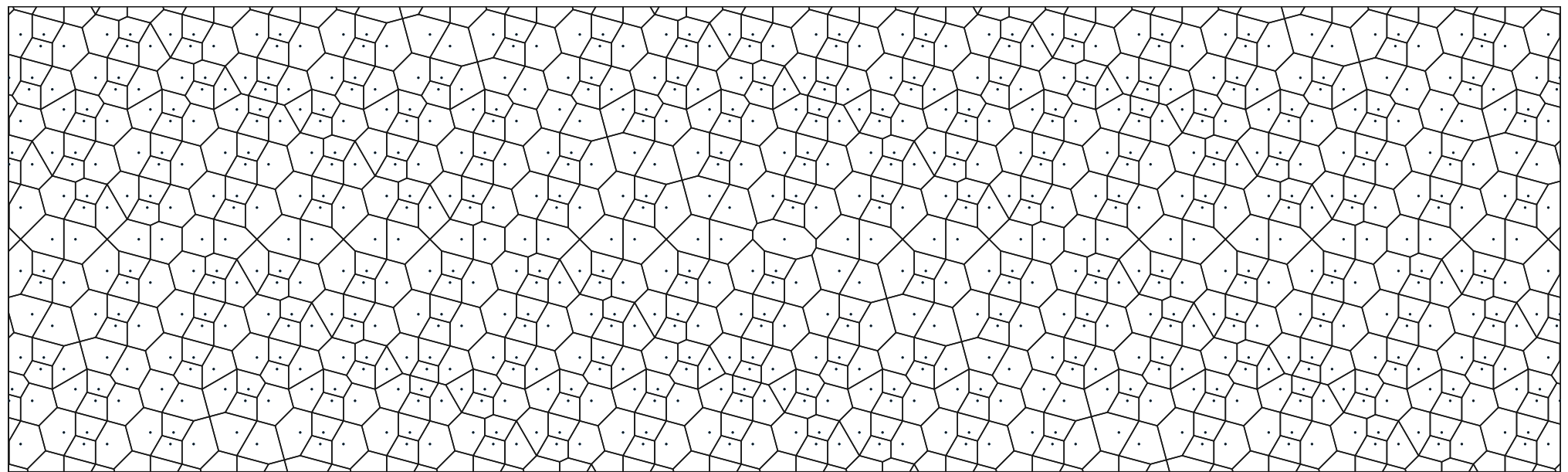
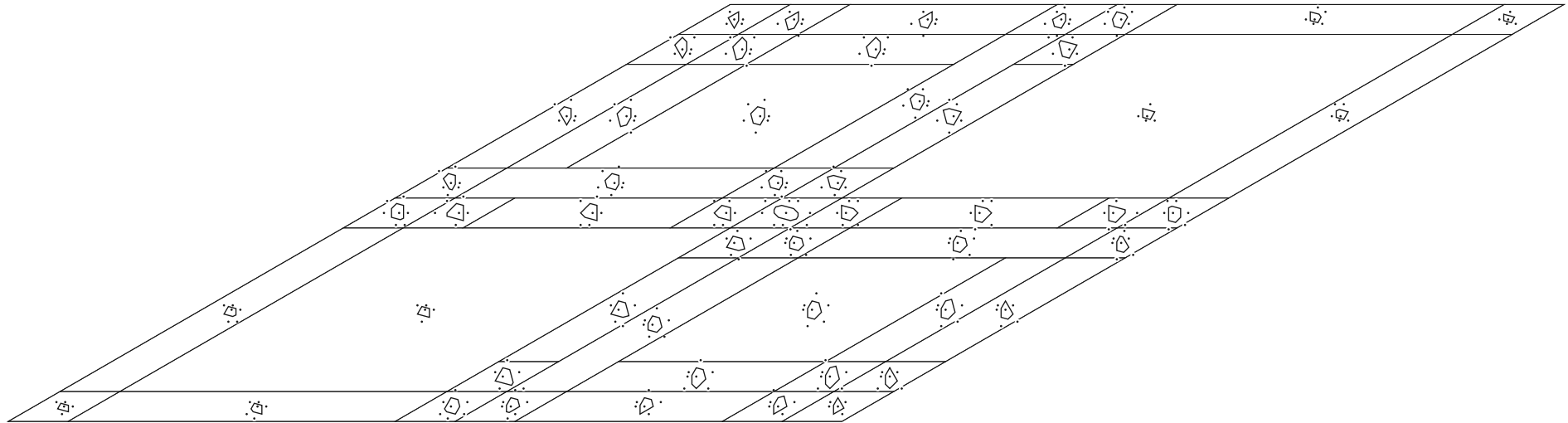
window size:  $6\beta - 22$



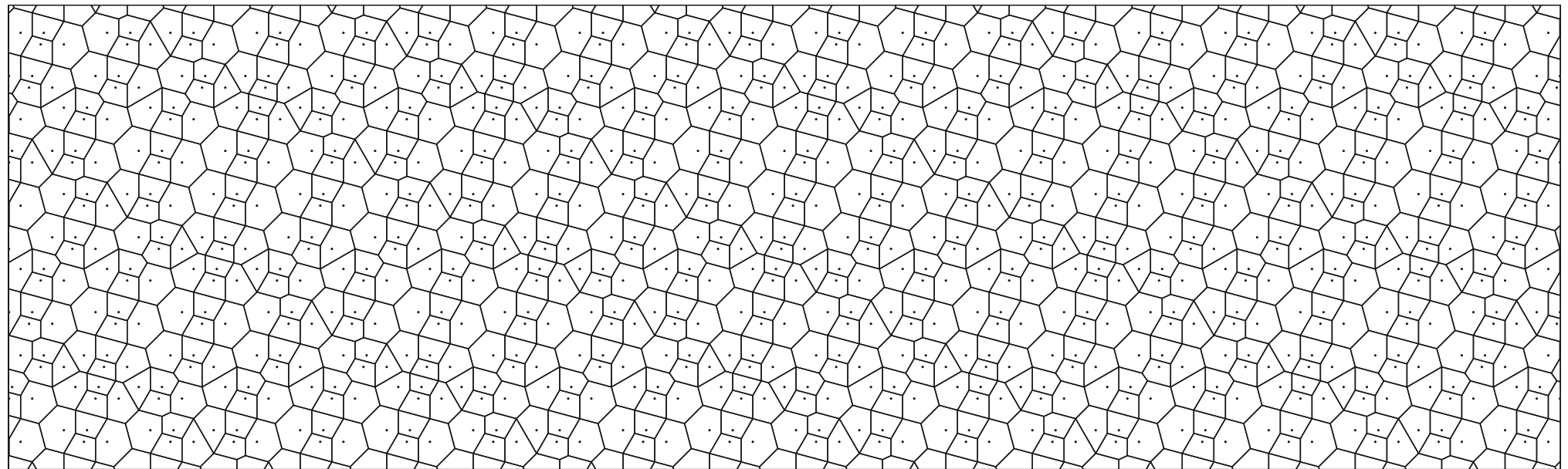
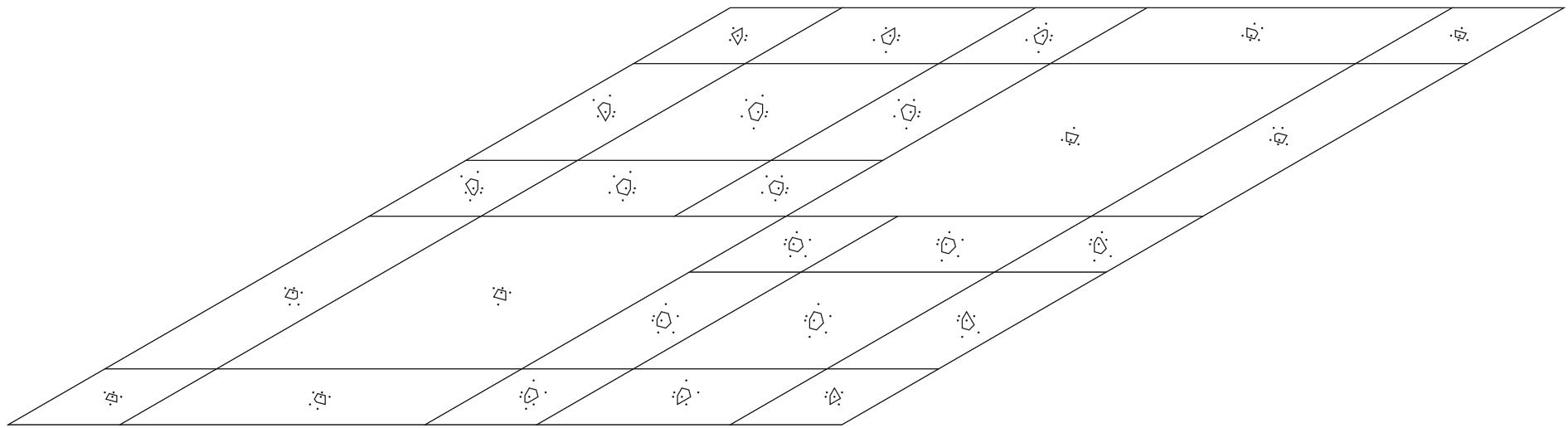
window size:  $\frac{8\beta-29}{2}$



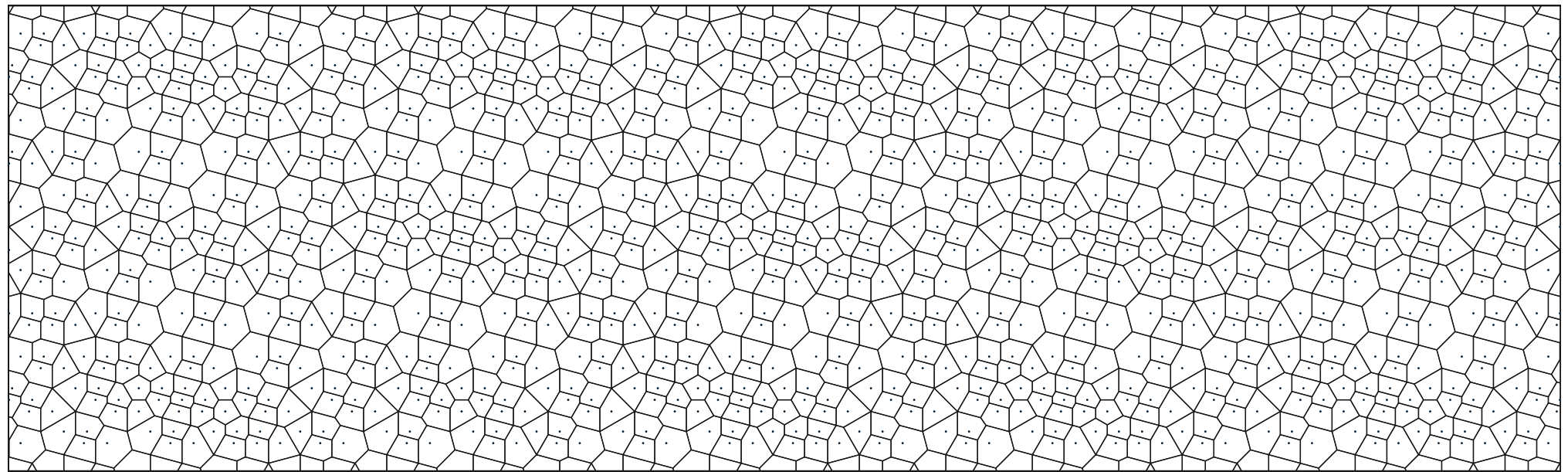
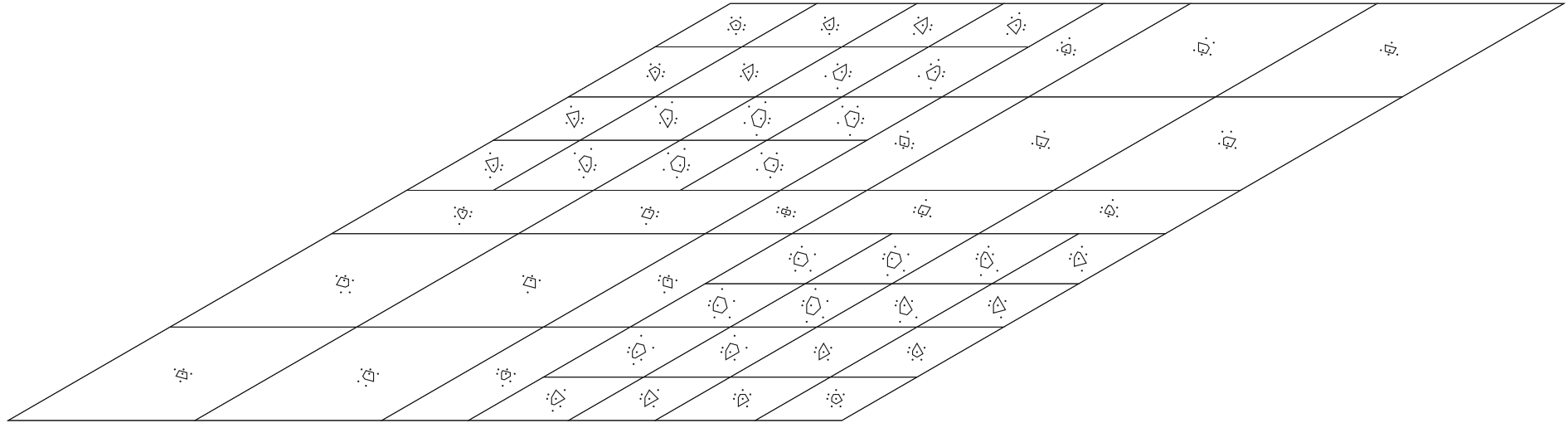
window size:  $2\beta - 7$



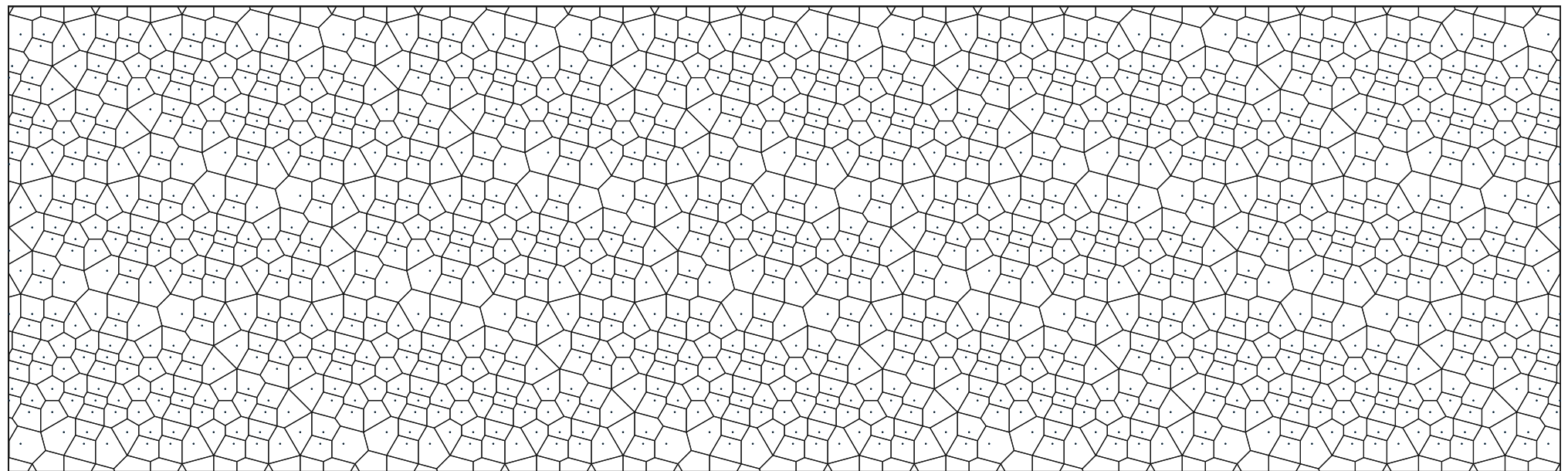
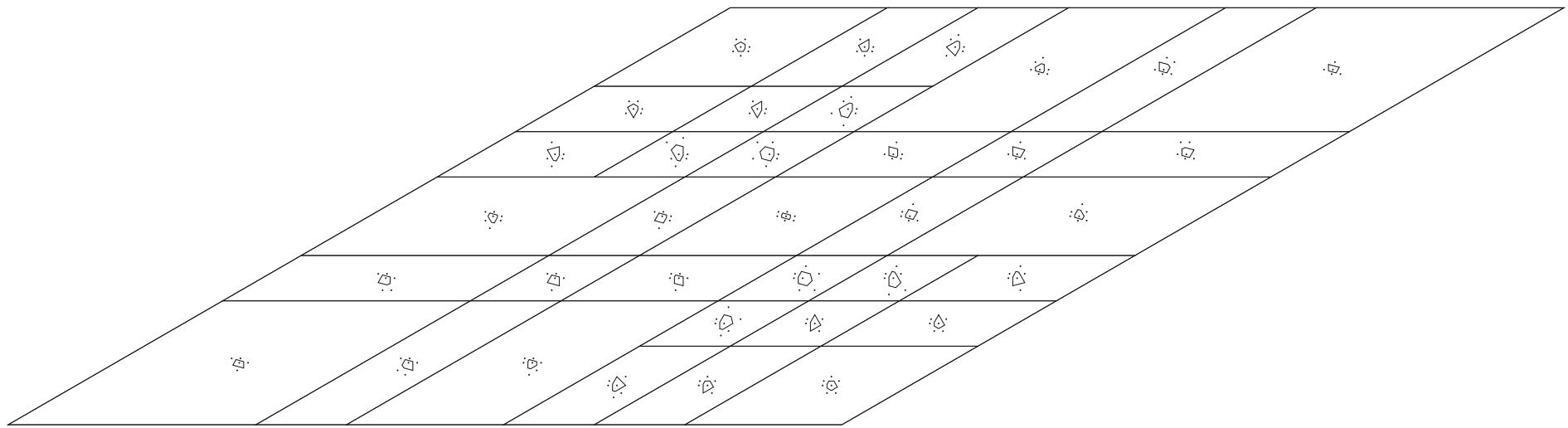
window size:  $\frac{1}{2}$



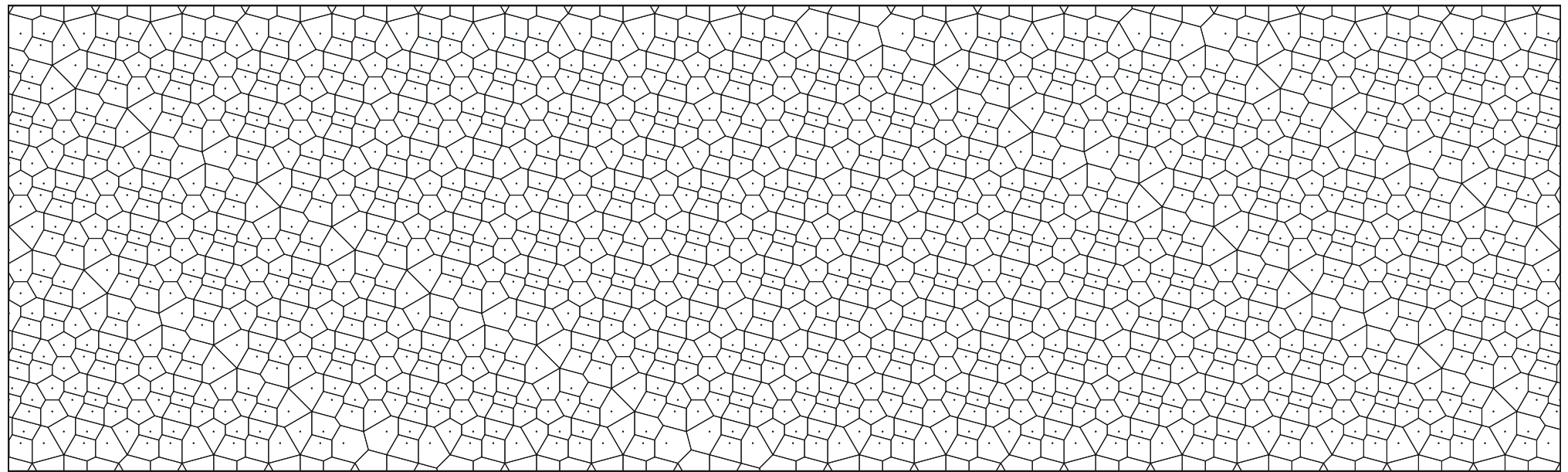
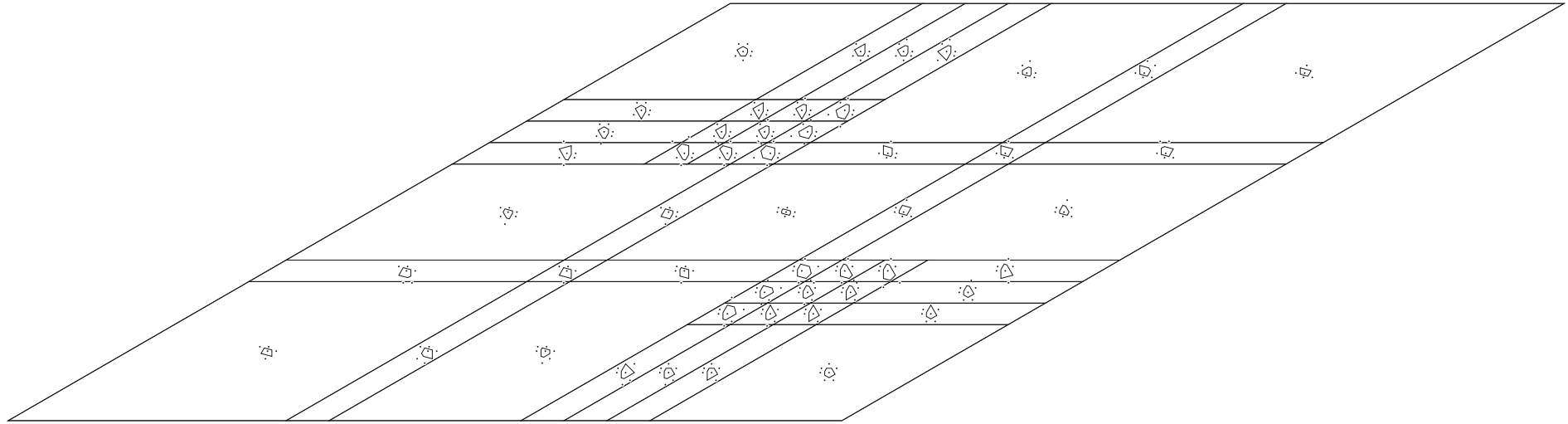
window size:  $8 - 2\beta$



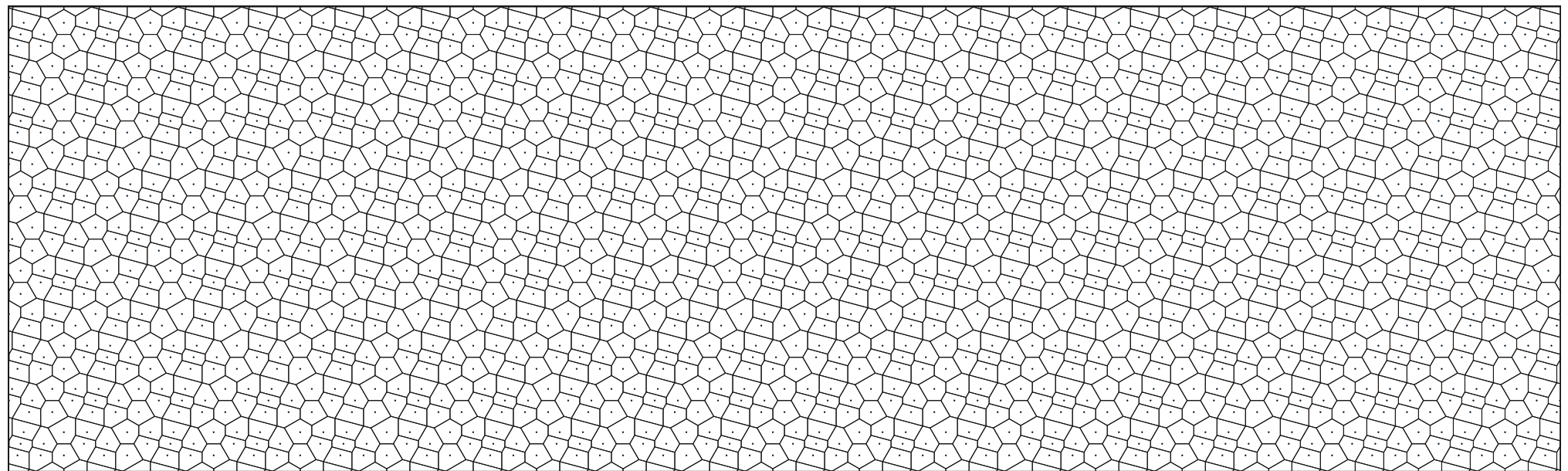
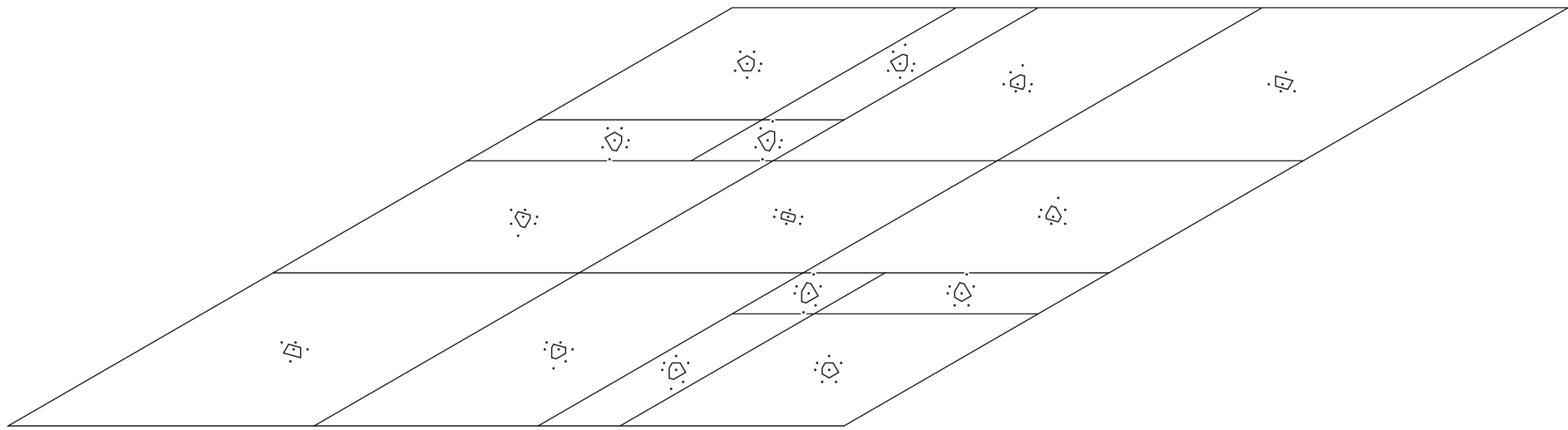
window size:  $\frac{3\beta-10}{2}$



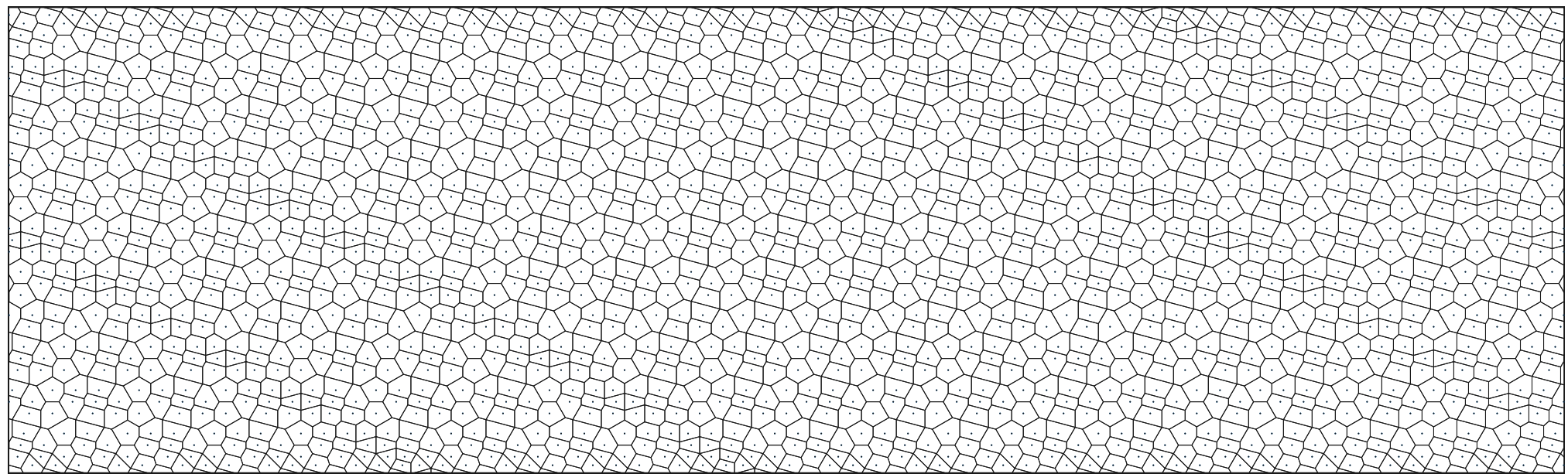
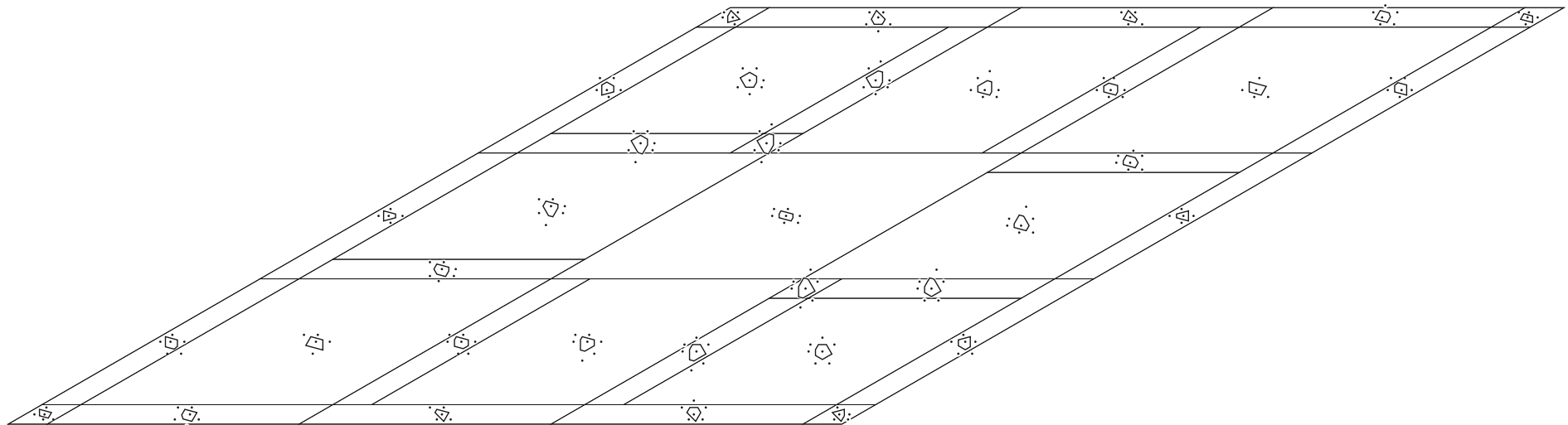
window size:  $5\beta - 18$



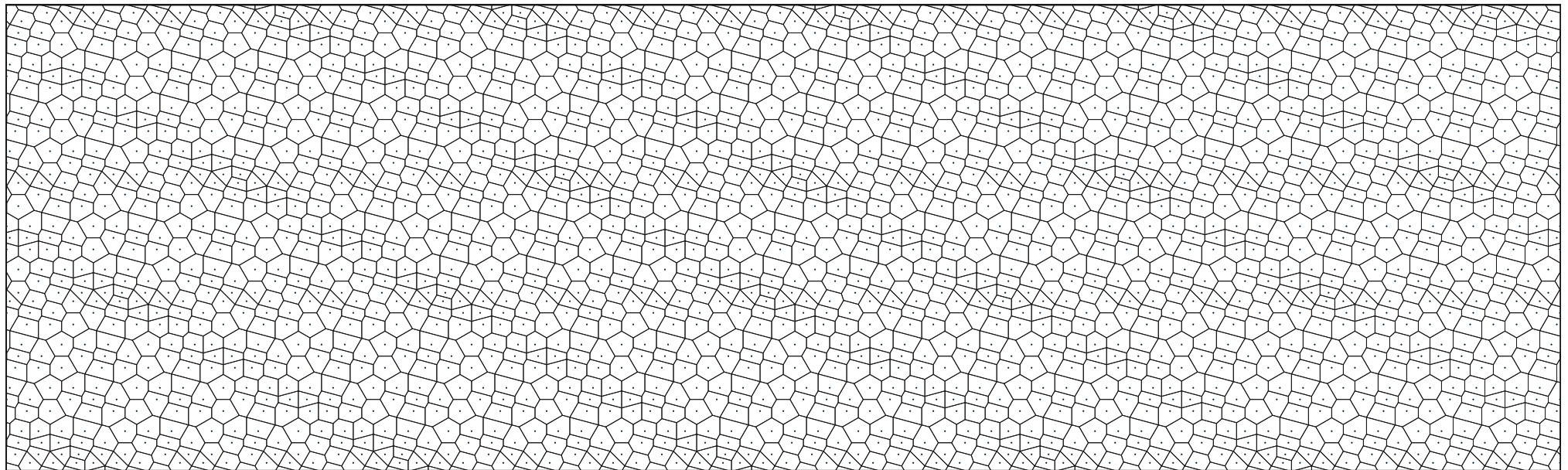
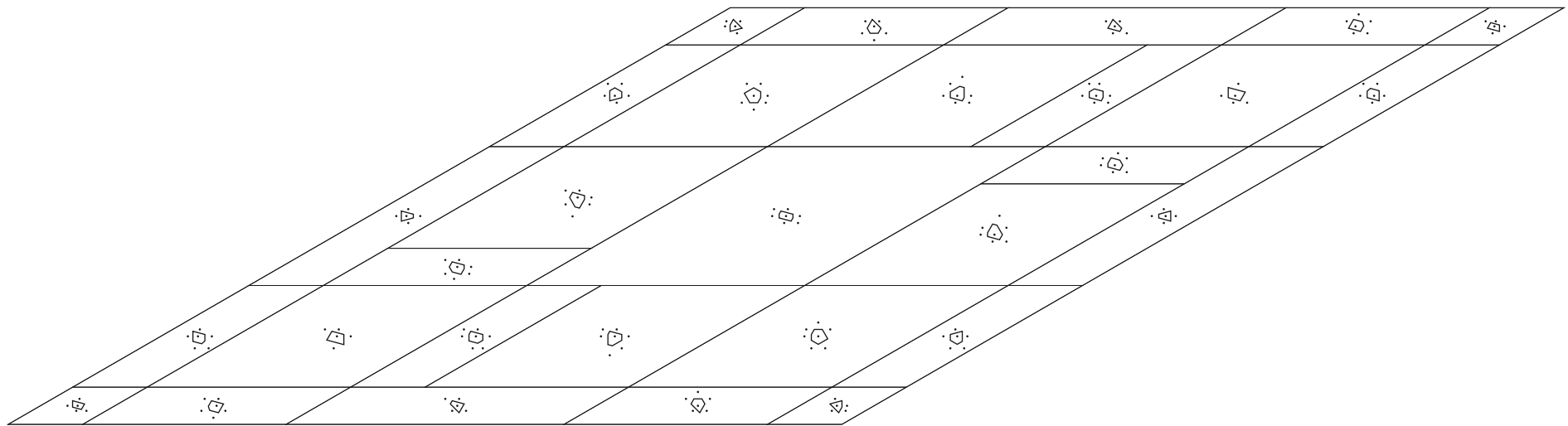
window size:  $\frac{6\beta-21}{2}$



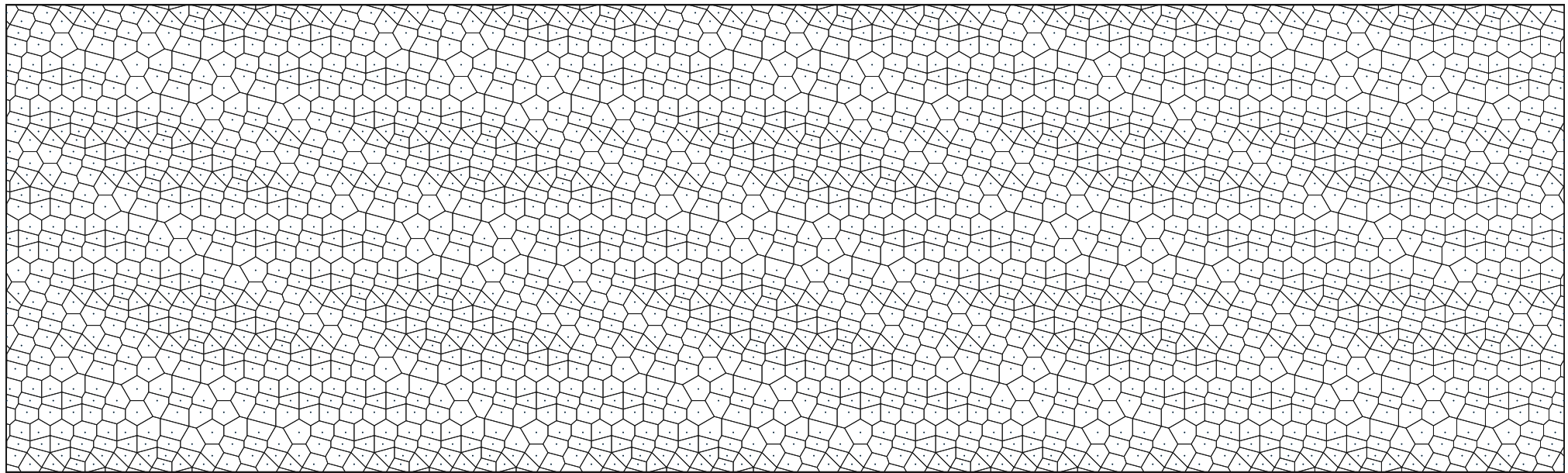
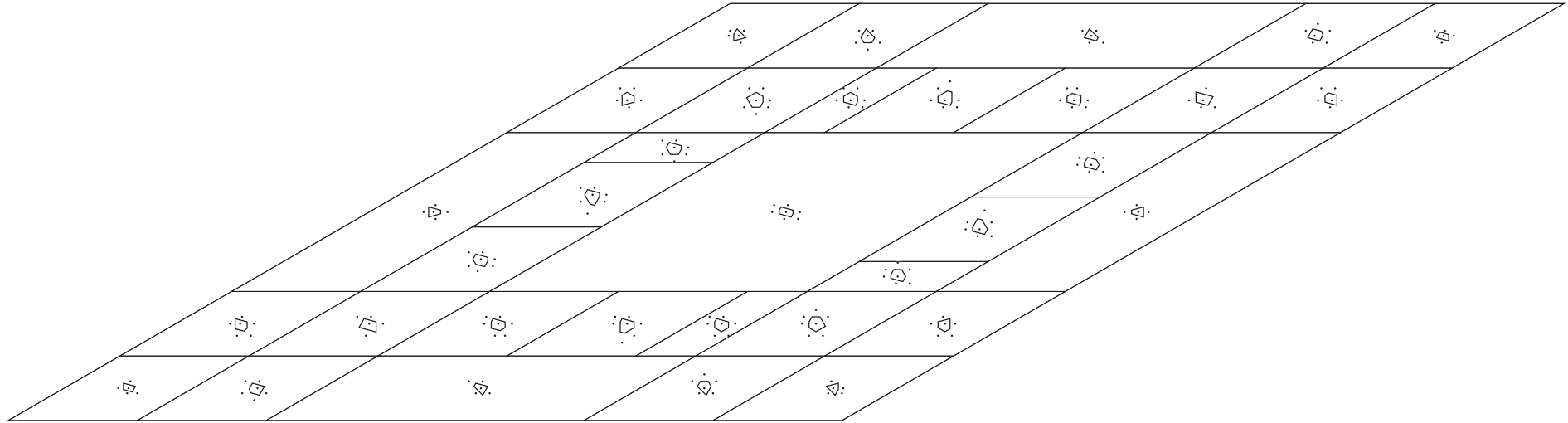
window size:  $\beta - 3$



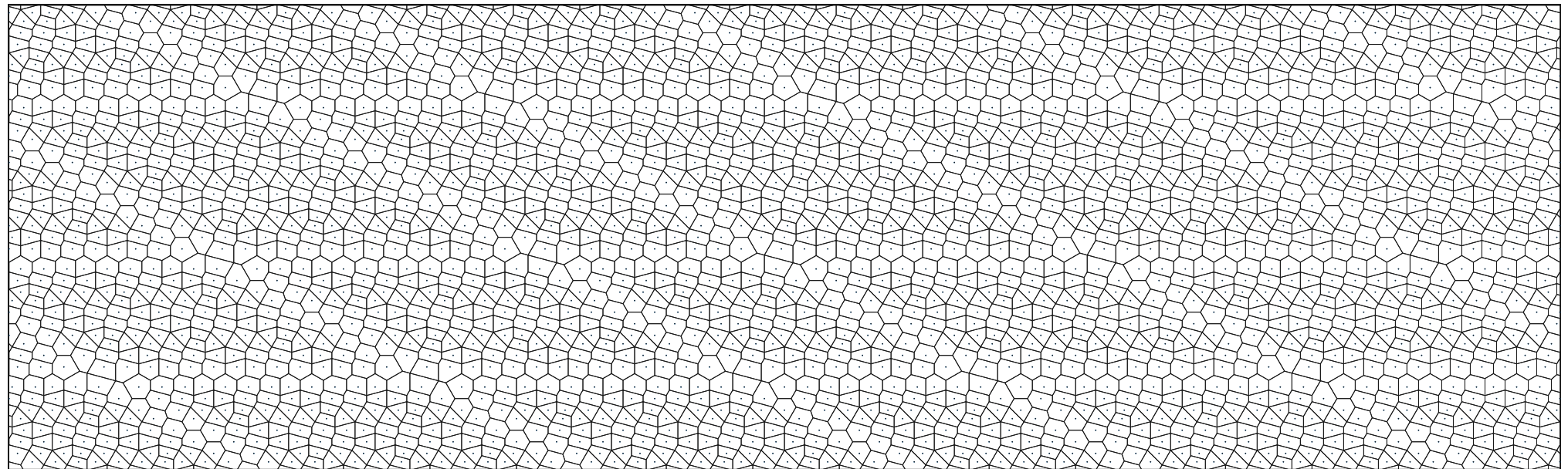
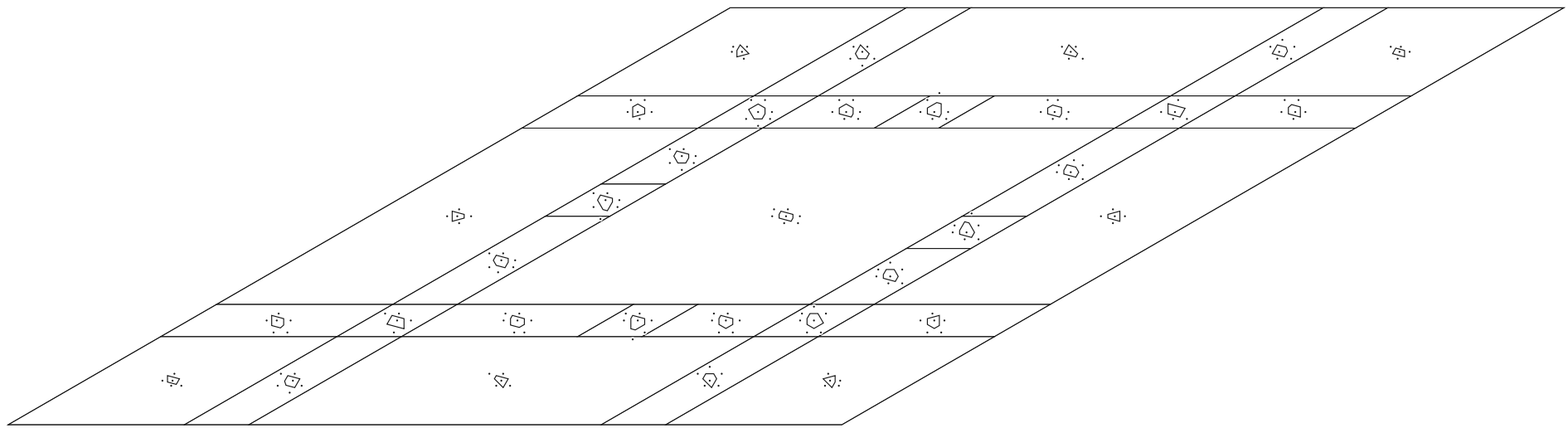
window size:  $\frac{9-2\beta}{2}$



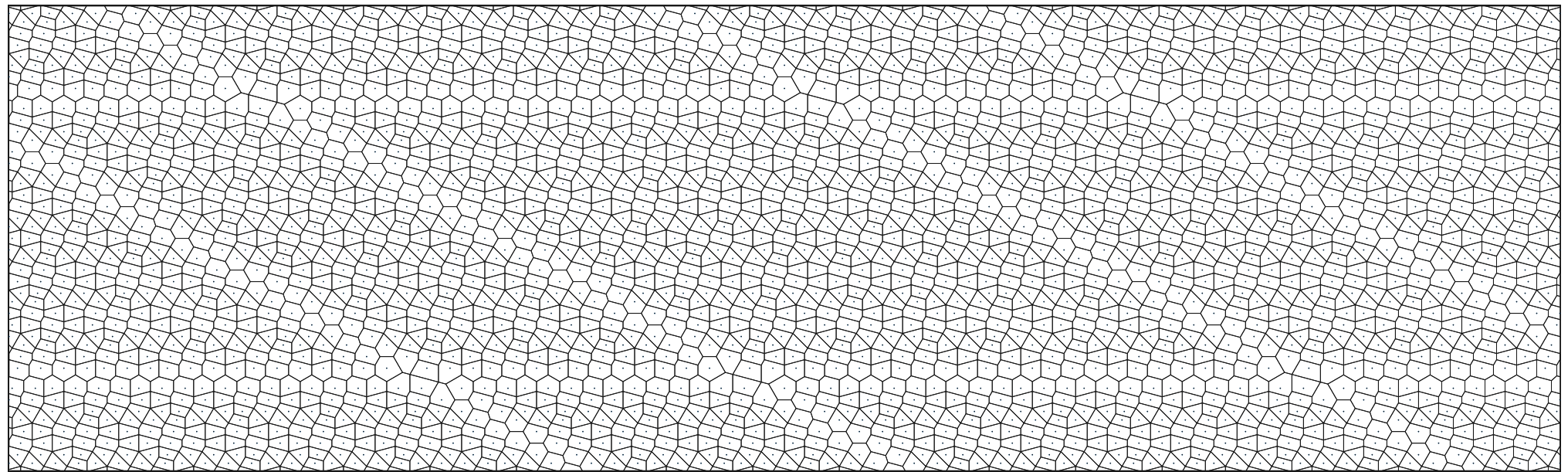
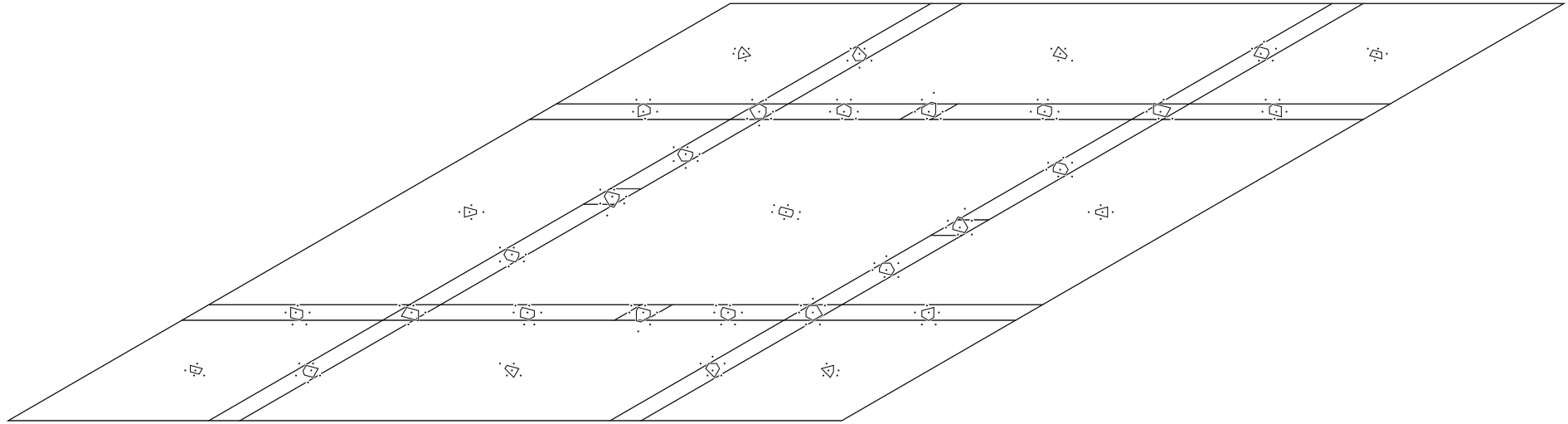
window size:  $12 - 3\beta$



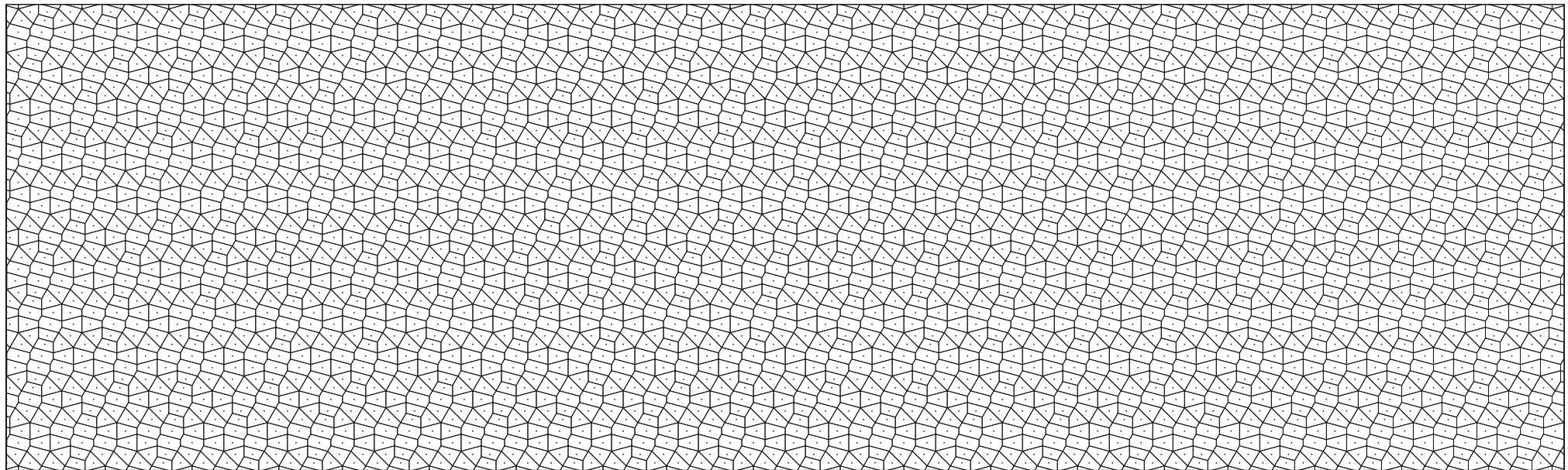
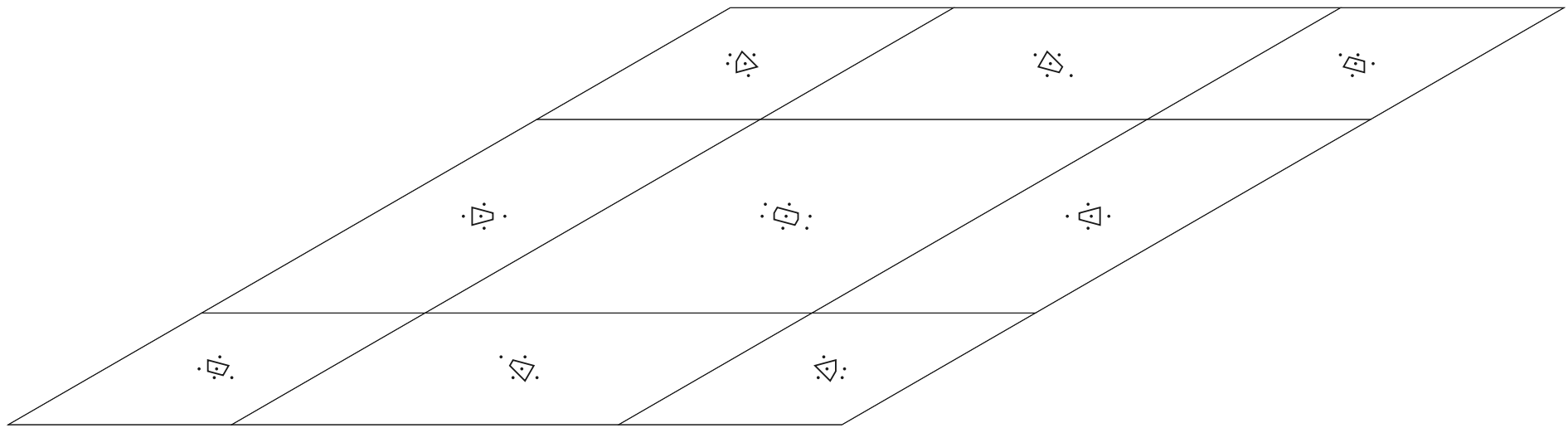
window size:  $\frac{\beta-2}{2}$



window size:  $4\beta - 14$



window size:  $\frac{4\beta-13}{2}$



window size: 1

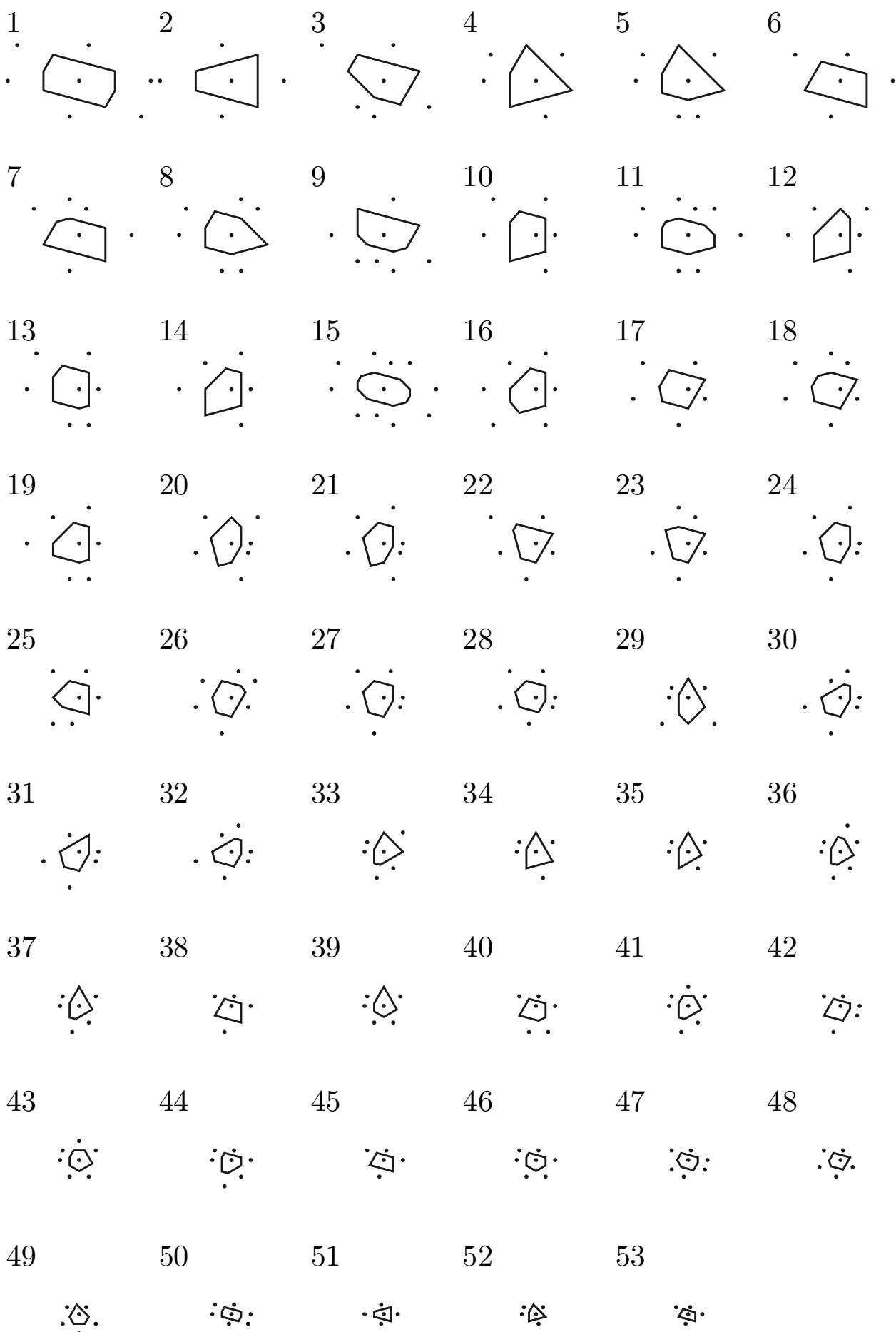


Figure 22: Catalog of all Voronoi polygons in quasicrystals with rhombic windows in the base form.

	1	2	3	4	5	6	7	8	9	10	11	12	13	14	15	16	17	18	19	20	21
1	•	•	•	•																	
2	•	•	•	•	•	•	•	•	•	•											
3		•	•	•	•																
4	•	•	•	•	•																
5		•	•	•	•																
6	•	•	•	•	•	•	•	•	•	•											
7		•	•	•	•	•	•	•													
8	•	•	•	•																	
9		•	•	•	•	•	•	•	•	•											
10	•	•	•	•	•	•	•	•	•	•	•										
11										•											
12	•	•	•	•	•	•	•	•	•	•	•	•	•	•	•	•	•	•	•	•	•
13					•																
14	•	•	•																		
15									•	•	•										
16									•												
17	•	•	•	•	•	•	•	•	•	•											
18									•	•	•										
19											•	•	•	•	•	•	•	•	•	•	•
20	•	•	•	•	•	•															
21						•	•	•	•	•	•										
22							•	•	•	•											
23							•	•	•	•											
24						•	•	•	•	•	•	•	•	•	•	•					
25										•											
26										•											
27										•	•	•									
28										•	•	•	•	•	•	•	•	•	•	•	•
29										•											
30										•	•	•	•	•	•	•	•	•	•	•	•
31										•	•	•	•	•	•	•	•	•	•	•	•
32																•					
33											•	•	•	•	•	•	•	•	•	•	•
34												•									
35											•	•	•	•	•	•	•	•	•	•	•
36																•	•	•	•	•	•
37																•	•	•	•	•	•
38	•	•	•	•	•	•	•	•	•	•	•	•	•	•	•	•	•	•	•	•	•
39																•	•	•	•	•	•
40											•	•	•	•	•	•	•	•	•	•	•
41																•	•	•	•	•	•
42												•	•	•	•	•	•	•	•	•	•
43												•	•	•	•	•	•	•	•	•	•
44												•	•	•	•	•	•	•	•	•	•
45												•	•	•	•	•	•	•	•	•	•
46																		•	•	•	•
47																•	•	•	•	•	•
48																•	•	•	•	•	•
49																•	•	•	•	•	•
50																•	•	•	•	•	•
51																•	•	•	•	•	•
52																•	•	•	•	•	•
53																•	•	•	•	•	•

Table 2: Assignment of Voronoi polygons to their quasicrystals. Horizontal axis enumerates members of  $\mathcal{D}$  and the vertical axis corresponds to the numbers from the list of Voronoi polygons (Figure 22).



## 10 Generation of finite section of quasicrystal with general window

Previous section concluded the analysis of a quasicrystal with a rhombic window. Now the results are applied to the analysis of quasicrystals with a window of a general shape.

Once again first an algorithm for generating a finite section of a quasicrystal with a general window is presented.

A property from Remark 16 (Theorem 2.3) is a key to such algorithm:

$$\Omega \subset \tilde{\Omega} \Rightarrow \Sigma(\Omega) \subset \Sigma(\tilde{\Omega})$$

To a given general window  $\Omega$  a rhombus window  $\hat{\Omega}$  is circumscribed. Therefore  $\Omega \subset \hat{\Omega}$ . Such window  $\hat{\Omega}$  is called the hyper-window and the quasicrystal  $\Sigma(\hat{\Omega})$  is called the hyper-quasicrystal.

Then a finite section of the hyper-quasicrystal  $\Sigma(\hat{\Omega})$  is constructed as described in previous sections and each point  $x \in \Sigma(\hat{\Omega})$  is individually tested whether  $x^* \in \Omega$ . Points that fail the test are discarded and the rest creates a finite section of the quasicrystal  $\Sigma(\Omega)$ .

To illustrate the algorithm a special kind of quasicrystal is presented. Its window is in the shape of an E and it is called Eduard.

Such algorithm can be applied to a window of literally any shape as long as a rhombus can be circumscribed. The natural next step is to catalog all different Voronoi polygons for all sizes of given general window. That is however significantly more complex than for a rhombic window.

## 11 Cataloging Voronoi polygons for fixed general window

The step from cataloging Voronoi polygons for a fixed rhombic window to cataloging Voronoi polygons for a single general window is significantly larger than the step from generating finite sections for a rhombic window to a general window described in the previous section.

The goal is again to generate all possible finite sections of the quasicrystal with a general window that cover a circle of the covering radius.

For that an opposite of the hyper-quasicrystal needs to be defined. To given general window  $\Omega$  a rhombic window  $\underline{\Omega}$  is inscribed. Therefore  $\underline{\Omega} \subset \Omega$ . The window  $\underline{\Omega}$  is called the hypo-window and the quasicrystal  $\Sigma(\underline{\Omega})$  is called the hypo-quasicrystal.

$$\underline{\Omega} \subset \Omega \subset \hat{\Omega} \quad \Rightarrow \quad \Sigma(\underline{\Omega}) \subset \Sigma(\Omega) \subset \Sigma(\hat{\Omega})$$

The hypo-quasicrystal creates a subset of the quasicrystal and the hyper-quasicrystal creates a superset. In other words the points of the hypo-quasicrystal are always present in the quasicrystal and the presence of the points of the hyper-quasicrystal needs to be decided. That is the key idea for the algorithm.

*Remark 22.* One-dimensional hyper-window means a one-dimensional window of the same size as is the size of the two-dimensional rhombic hyper-window. Equivalently for the hypo-window.

### Algorithm

1. estimate the covering radius from the hypo-quasicrystal (it is certainly larger than the one for the quasicrystal)

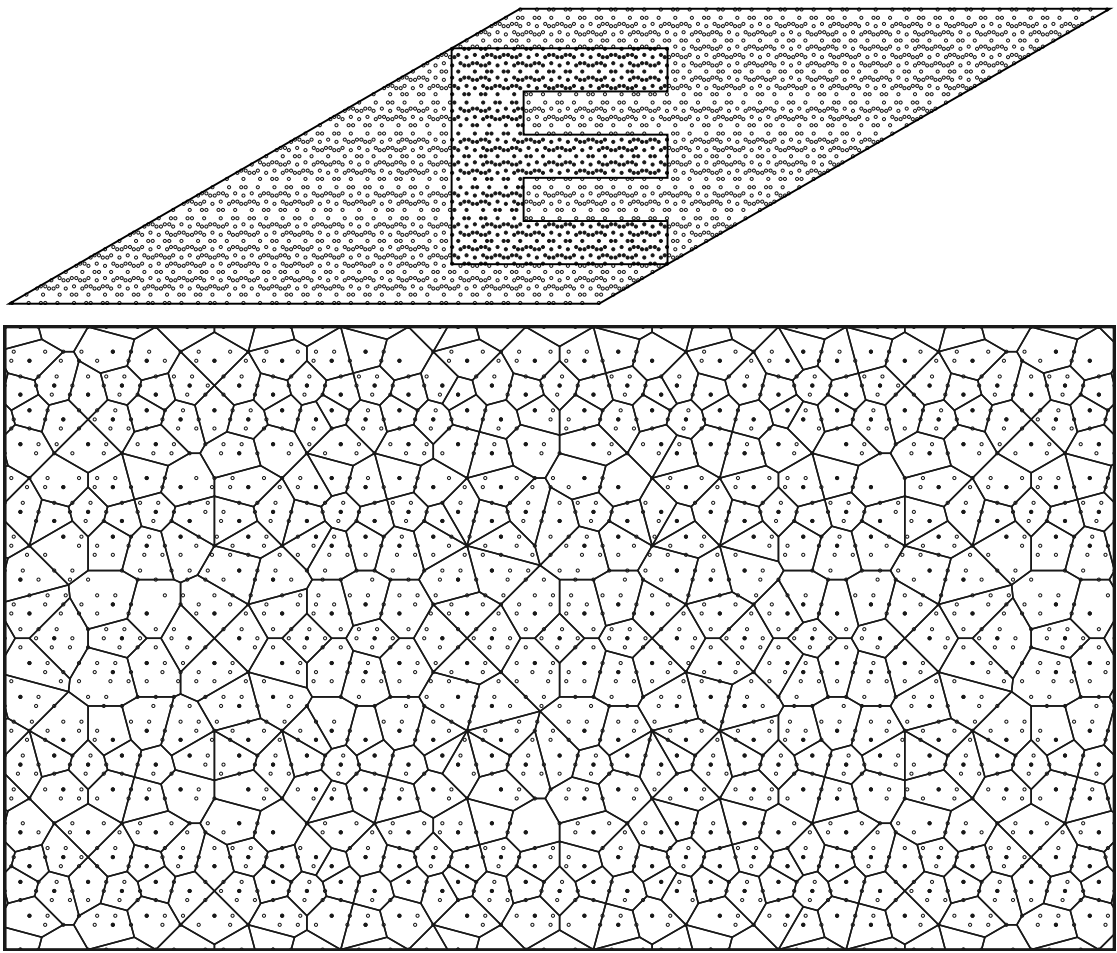


Figure 23: Illustration of the algorithm for generating a finite section of a quasicrystal with a general window. The top image displays a window in the shape of an  $\mathbb{E}$  its hyper-window and the \* images of points of the quasicrystal Eduard (full) and of points of the hyper-quasicrystal (empty). The lower image displays the quasicrystal Eduard (with Voronoi polygons) and the hyper-quasicrystal (only points).

2. estimate the sufficient  $n$  so that the finite section of the word of the hyper-quasicrystal covers the necessary distance
3. generate finite sections of the hyper-quasicrystal from the language of the sufficient  $n$
4. mark the points of the hypo-quasicrystal in each finite section
5. determine which of the unmarked points belong to the quasicrystal
6. construct Voronoi polygons
7. select Voronoi polygons that actually appear in the quasicrystal

## 11.1 Identifying the points of the hypo-quasicrystal

To take advantage of the hypo-quasicrystal its points need to be identified in the finite sections. The one-dimensional quasicrystal corresponding to the hypo-quasicrystal is a sparser subset of the one-dimensional quasicrystal corresponding to the hyper-quasicrystal.

The identification is started already while generating the language  $\mathcal{L}_\ell(n)$ . The algorithm for dividing a one-dimensional window is augmented. Output of the new algorithm is no longer a section of the word of the quasicrystal: every second letter is  $t_{2i} \in \{0, 1\}$  and it denotes whether the point after the distance represented by the previous letter is present in the one-dimensional quasicrystal corresponding to the hypo-quasicrystal.

At each step of the iteration the intervals are further divided by the one-dimensional hypo-window. As is presented in Figure 24.

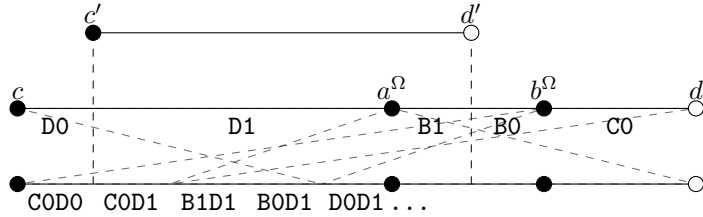


Figure 24: Illustration of creating words with the marks of belonging to the one-dimensional hypo-window. The one-dimensional hypo-window is displayed as the interval  $[c', d')$  and the one-dimensional hyper-window is displayed as the interval  $[c, d)$ .

While constructing the finite sections of the quasicrystal, points are marked once both letters are succeeded by 1. Finite section in Figure 25 was created from the following words.

`DOB0DOC0D0D1C0D0D1C0` and `C0D0B1DOB0D1C0D0D1C0`

The first letter is skipped and so the second letter determines the mark for the first points in the finite section. Therefore the finite section is smaller than the one for a rhombic window in previous section.

The set of unmarked points  $P = \Sigma(\widehat{\Omega}) \setminus \Sigma(\Omega)$  is called the potential of the finite section.

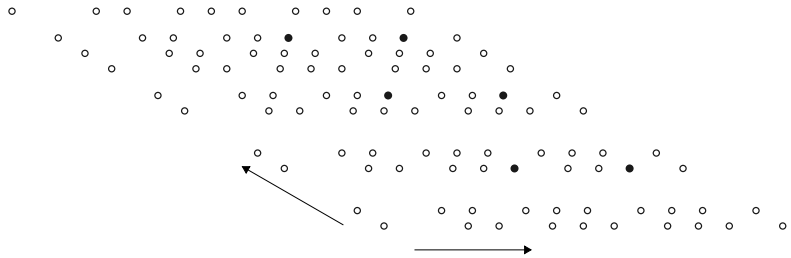


Figure 25: Finite section created from the words `DOB0DOC0D0D1C0D0D1C0` (horizontal) and `C0D0B1DOB0D1C0D0D1C0` (vertical). The points of the hypo-quasicrystal (full) and the potential (empty).

The next step is to determine which points of the potential belong to the quasicrystal  $\Sigma(\Omega)$ . In other words creating finite sections of the quasicrystal with a general window.

## 11.2 Finite sections of a quasicrystal with a general window

To acquire finite sections of the quasicrystal with a general window the finite sections of the hypo-quasicrystal and their potentials are processed individually.

Let  $F$  be the finite section and  $P \subset F$  is its potential. Clearly  $F \setminus P$  are the points of the hypo-quasicrystal and  $(F \setminus P)^* \subset \Omega \subset \Omega$ .

The points of the potential are considered one at a time. For each  $x \in P$  it needs to be tested whether  $((F \setminus P) \cup x)^*$  fits inside the window  $\Omega$ . Method for such test was already covered in previous section.

$$\begin{aligned} (F \setminus P) &= \{x_1, \dots, x_k\} \\ x^* \in \Omega \quad \wedge \quad x_i^* &\in \Omega \quad \forall i \in \hat{k} \\ q_i = x_i - x \quad \forall i &\in \hat{k} \\ x^* \in \Omega \quad \wedge \quad x^* + q_i^* &\in \Omega \quad \forall i \in \hat{k} \\ x^* \in \Omega \quad \wedge \quad x^* &\in \Omega - q_i^* \quad \forall i \in \hat{k} \\ x^* \in \bigcap_{i \in \hat{k}} (\Omega - q_i^*) \cap \Omega \end{aligned}$$

Therefore the test turns into whether is the intersection empty or not. If it is empty  $x$  is removed from both  $P$  and  $F$  if it is not empty  $x$  is only removed from  $P$ , thus becoming the point of the finite section  $F \setminus P$ .

In theory the finite section of the quasicrystal is a union of the finite section of the hypoquasicrystal and any number of points of its potential. As long as the union passes the test. There may even be more finite sections of the quasicrystal arising from a single finite section of the hypo-quasicrystal and its potential. Therefore the algorithm needs to test the fit for each subset of the potential and it branches into a tree structure, one branch for every remaining point of the potential. The computational complexity is huge.

Such process produces a superset of all finite sections of the algorithm, such finite sections that could appear in the quasicrystal. The next section presents a method of determining which finite sections actually do appear.

## 11.3 Voronoi polygons that actually appear in the quasicrystal

The Figure 26 illustrates the issue nicely. Both finite sections are results from the algorithm from the previous section. Depending on the shape of the window the second one may fit in the window every time the first one does. That would imply that the first polygon never appears in the quasicrystal since it would always be cut to the smaller second one.

Solution was also partially covered while analyzing the quasicrystals with a rhombic window.

Once a Voronoi polygon is created for each finite section only the domain of the polygon is kept and the rest is discarded.

The intersection is constructed as before: Let  $V$  be one of the Voronoi polygons in the quasicrystal,  $c$  the center of  $V$ ,  $D = \{p_1, \dots, p_k\}$  the domain of  $V$  and  $q_i = p_i - c$ ,  $i \in \hat{k}$ .

$$Q = \bigcap_{i \in \hat{k}} (\Omega - q_i^*) \cap \Omega$$

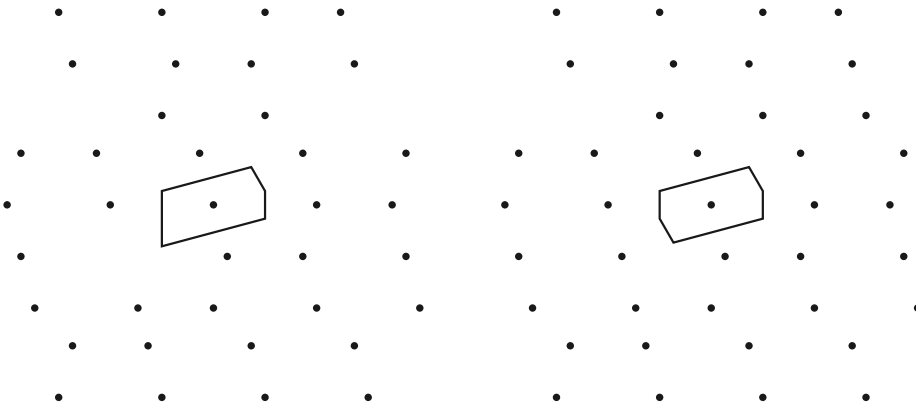


Figure 26: Example of two Voronoi polygons constructed over two finite sections from the algorithm from the previous section.

Once  $c^* \in Q$  then the domain of  $V$  appears in the quasicrystal. For different Voronoi polygons these intersections may overlap. However unlike for a rhombic window, for a general window some intersections may get entirely covered by intersections of other Voronoi polygons and thus eliminating the corresponding Voronoi polygon from the quasicrystal.

To determine which Voronoi polygons actually appear in the quasicrystal the intersection of all candidate Voronoi polygons need to be stacked up sorted from the smallest Voronoi polygon on the top and the polygons whose intersections are entirely coved are eliminated. Thus a catalog of Voronoi polygons for a fixed quasicrystal with a general window is created.

## 12 Cataloging Voronoi polygons for all sizes of general window

Same as with the rhombic window the goal is to pick several fixed sizes of the window whose Voronoi polygons catalogs cover the global Voronoi polygon catalog. Solution comes from the idea that while increasing the size of the window linearly, the sizes of the hyper-window and hypo-window also grow linearly. Of course these windows are rhombi and have properties from Theorem 2.3.

$$\Sigma(\beta\Omega) = \frac{1}{\beta} \Sigma(\Omega)$$

Thus the interval  $(\frac{1}{\beta}, 1]$  is divided by the length of the word into intervals and any one size is analyzed from within each interval.

The next section will apply these findings to a circle.

## 13 Analysis of a quasicrystal with a circular window

The methods for analysis of a general window from the previous section can be applied to the analysis of a circular window. First the hyper-window and the hypo-window need to be

established.

The quasicrystals based on the irrationality  $\beta$  do intrinsically posses twelve-fold rotational symmetry. However this symmetry is only realized when the window posses twelve-fold rotational symmetry also. Which a circle naturally does.

Formulas for inscribing and circumscribing a rhombus to a circle are rather simple,  $\hat{\ell}$  and  $\ell$  denote the sizes of the hyper-window and the hypo-window respectively,  $R$  denotes the radius of the circle.

$$\hat{\ell} = 4R \quad \ell = \frac{15 - 3\beta}{4}R$$

The value for  $\ell$  is actually an estimate. Precise formula contains  $\sqrt{2}$  which is estimated by  $6\beta - 21 \doteq 1.3923 < 1.4142 \doteq \sqrt{2}$  (unlike before this is a low estimate). The hypo-window is thus slightly smaller however unlike  $\sqrt{2}$ ,  $\ell \in M$ .

With the hyper-window established, it is trivial to construct finite sections of a quasicrystal with a circular window.

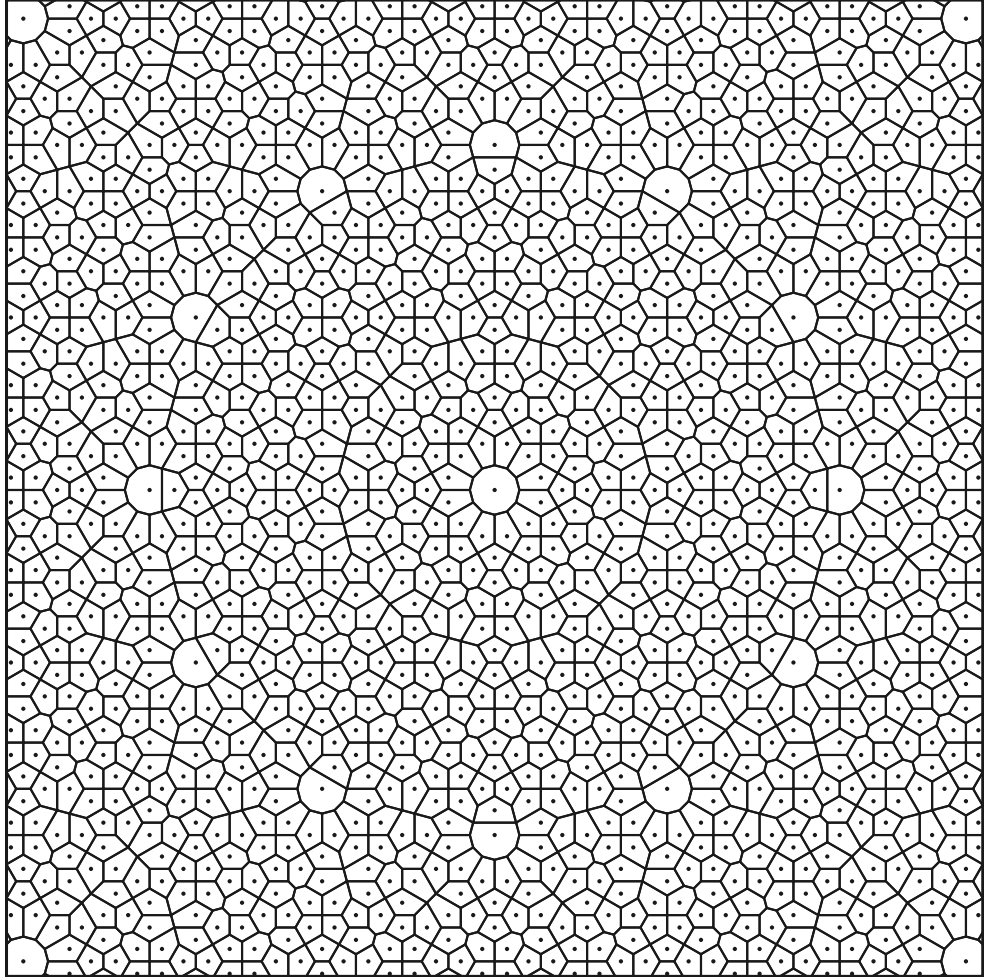


Figure 27: Example of a finite section of a quasicrystal with a circular window (note the twelve-fold rotational symmetry).

However once attempting to catalog the voronoi polygons the computation was never able to finish neither memory-wise nor time-wise. Therefore the aim of further work is to parallelize the program and properly finish the analysis of quasicrystals with circular windows.

## Computation

It should not be a surprise that most of the analysis is done with a computer programs. These programs were not yet discussed since they are a literal transcriptions of the described algorithms. There are two concepts that make it possible: precise arithmetic in  $\mathbb{Q}(\beta)$  and object-oriented programming.

### 13.1 Precise arithmetic in $\mathbb{Q}(\beta)$

Nearly every calculation in the algorithms is inside the number field  $\mathbb{Q}(\beta)$ . It is possible to implement a custom class that will enable precise calculations. Since  $\beta$  is quadratic the field has the following simple form.

$$\mathbb{Q}(\beta) = \left\{ \frac{a + b\beta}{c} \mid a, b \in \mathbb{Z}, c \in \mathbb{N} \right\}$$

Therefore each number  $x \in \mathbb{Q}(\beta)$  can be represented by three integers and integer arithmetic is precise. Several operations are listed here. Particularly useful is the `simplify` function which makes sure that  $a, b, c$  do not overflow. (`gcd` returns the greatest common divisor)

### 13.2 Object-oriented programming

Many objects were implemented to represent various structures used in the algorithms: `Cpoint`, `CpointSet`, `CDeloneSet`, `CVoronoiCell` and more. Such abstraction truly allows a literal transcription of the algorithms as they are explained in the text.

If you are interested in diving into the code yourself, every program used to make this text is available online: <https://github.com/edasubert/quasicrystal>

The algorithms and programs for the golden ratio variant of quasicrystal are described in great detail in [6].

---

**Algorithm 1:** Precise arithmetic inside  $\mathbb{Q}(\beta)$ .

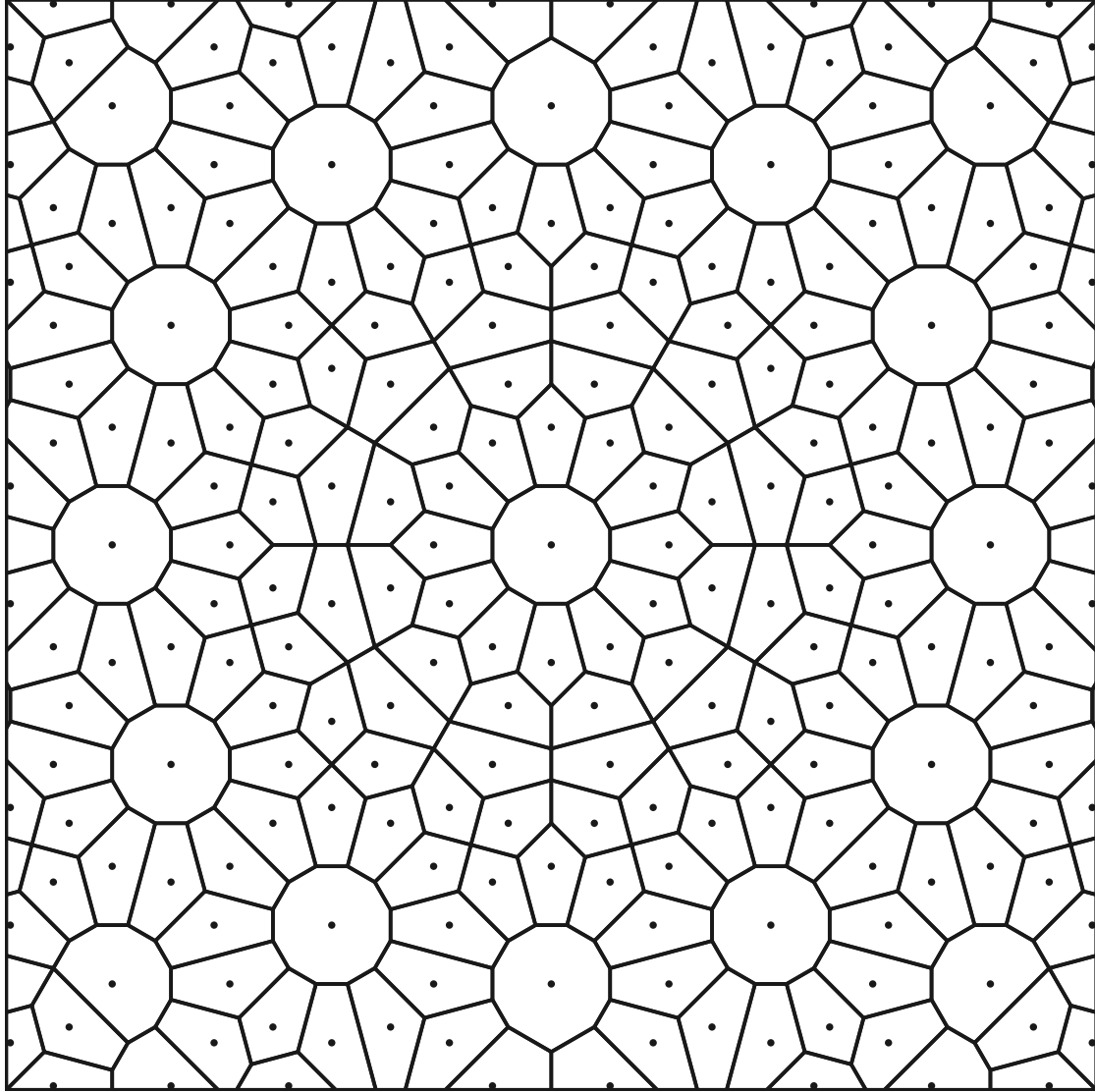
---

```
Function operator + (p,q)
1   p.a = p.a*q.c + q.a*p.c;
2   p.b = p.b*q.c + q.b*p.c;
3   p.c = p.c * q.c;
4   return p;
Function operator * (p,q)
1   p.a = p.a*q.a - p.b*q.b;
2   p.b = p.b*q.a + p.a*q.b + 4*p.b*q.b;
3   p.c = p.c * q.c;
4   return p;
Function operator / (p,q)
1   p.a = (p.a*q.a + p.b*q.b + 4*p.a*q.b)*q.c;
2   p.b = (p.b*q.a - p.a*q.b)*q.c;
3   p.c = (q.a*q.a + 4*q.a*q.b + q.b*q.b)*p.c;
4   return p;
Function operator < (p,q)
1   A = p.a*q.c+p.b*q.c*2 - q.a*p.c-q.b*p.c*2;
2   B = q.b*p.c - p.b*q.c;
3   if sign(A)*A*A < 3*sign(B)*B*B then
4       | return true;
5   end
5   return false;
Function simplify(p)
1   cache = 0;
2   if ((cache = gcd(a,b)) != 0) && ((cache = gcd(cache,c)) != 0) && (cache > 1 ) then
3       | p.a = p.a/cache;
4       | p.b = p.b/cache;
5       | p.c = p.c/cache;
6   end
6   return p;
```

---

## Conclusion

This work presented mostly the theoretical preparation for the analysis of the quasicrystals with a circular window. The analysis is however not yet concluded and so it will be subject of future work. That leaves enough space for a nice quasicrystal with a dodecagonal window which also posses twelve-fold rotational symmetry and also will be a part of the future work.



## References

- [1] Z MASÁKOVÁ, J PATERA a J ZICH. *Classification of Voronoi and Delone tiles in quasicrystals. I. General method.* J. Phys. A **36** (2003), 1869–1894.
- [2] Z MASÁKOVÁ, J PATERA a J ZICH. *Classification of Voronoi and Delone tiles of quasicrystals: II. Circular acceptance window of arbitrary size* J. Phys. A **36** (2003), 1895–1912.
- [3] Z MASÁKOVÁ, J PATERA a J ZICH. *Classification of Voronoi and Delone tiles of quasicrystals: III. Decagonal acceptance window of any size* J. Phys. A **38** (2005), 1847–1960.
- [4] L-S GUIMOND, Z MASÁKOVÁ, E PELANTOVÁ. *Combinatorial properties of infinite words associated with cut-and-project sequences.* J. Théor. Nombres Bordeaux **15** (2003), 697–725.
- [5] J.-P. GAZEAU. *Pisot-cyclotomic integers for quasilattices* in: The mathematics of long-range aperiodic order (Waterloo, ON, 1995), Kluwer Academic Publishers, Dordrecht, (1997), pp. 175–198.
- [6] J ZICH. *Voronoi & Delone tiling of quasicrystals.* Fakulta jaderná a fyzikálně inženýrská České vysoké učení technické v Praze, 2002. Diplomová práce. Vedoucí práce Z Masáková.
- [7] E ŠUBERT. *Voronoiova dláždění a Cut-and-Project množiny.* Fakulta jaderná a fyzikálně inženýrská České vysoké učení technické v Praze, 2014. Bakalářská práce.